FACULTY OF ENGINEERING OF THE UNIVERSITY OF PORTO

Comparison of the arterial blood pressure digital signal acquired using invasive and non-invasive methods

Raquel Pires Alves

MSc DISSERTATION

Integrated Master in Bioengineering - Biomedical Engineering

Supervisor: PhD. Teresa Henriques

Co-supervisor: PhD. João Paulo Cunha

June 28, 2020

Comparison of the arterial blood pressure digital signal acquired using invasive and non-invasive methods

Raquel Pires Alves

Integrated Master in Bioengineering - Biomedical Engineering

June 28, 2020

Resumo

A pressão arterial é um sinal vital com relevância clínica significativa, uma vez que está relacionada com mortalidade por causas vasculares ou diversos riscos cardíacos.

O *ClearSight System* é um sistema que incorpora um dispositivo Nexfin® e mede inúmeros parâmetros hemodinâmicos de forma contínua através de um sensor de absorção de luz e uma braçadeira de dedo inflável. Este método surgiu como uma alternativa aos métodos invasivos para monitorizar a pressão arterial continuamente evitando as complicações associadas à colocação de um catéter, como sangramento, infecção ou isquemia.

Vários estudos foram realizados para validar a usabilidade do dispositivo Nexfin®, comparando-o com métodos certificados e utilizados clinicamente. Essas comparações são baseadas na variação de valores isolados, como valores de pressão arterial média, pressão sistólica e diastólica, débito cardíaco ou índice cardíaco ao longo do tempo.

Este trabalho pretende a validação do dispositivo *ClearSight System* através da análise da dinâmica das séries temporais de sinais adquiridos continuamente. O objetivo é caracterizar o sinal sincronizado de 14 pacientes submetidos a cirurgia cardíaca. Os dados de pressão arterial foram recolhidos para cada sujeito com técnicas invasivas e não invasivas. As duas séries temporais foram comparadas usando os métodos lineares, de tempo e frequência, e não lineares, incluindo medidas estatísticas, espectrais e de complexidade, como a entropia e a compressão. A correlação das medidas obtidas com os índices de risco também foi analisada.

Foram encontradas diferenças entre os sinais adquiridos pelos dois métodos para todos os índices. Contudo, muitos dos parâmetros apresentam correlações moderadas a elevadas. A correlação das medidas obtidas com os índices de risco também foi analisada.

Os resultados obtidos demonstram que o dispositivo Nexfin® capta a dinâmica das séries temporais de pressão arterial. Além disso, os sinais obtidos pelo método não invasivo relacionam-se com os valores de risco. Em particular, os índices de entropia são associados inversamente com o risco de morbilidade e mortalidade da STS e os índices de compressão são inversamente associados com o tempo que o paciente passou nos cuidados intensivos.

Os resultados sugerem que os dados de pressão arterial recolhidos pelo Nexfi® do *ClearSight System* mantêm as dinâmicas lineares e não lineares dos dados e são correlacionados com os índices de risco cardiovascular.

Abstract

Blood Pressure (BP) is one vital sign with significant clinical relevance once its information can be related to vascular mortality or cardiac risks.

The *ClearSight system* is a setup that incorporates a Nexfin® device, and that measure numerous hemodynamic parameters continuously through a light-absorption sensor and an inflatable finger cuff. It emerged as an alternative to the invasive methods to continuously monitor the blood pressure since it avoids the complications associated with catheter placement such as bleeding, infection, or ischemia.

Several studies have been conducted towards the validation of the usability of the Nexfin method by comparing it with certified and clinically used methods. These comparisons are based on the variation of isolated values such as mean arterial pressure, systolic and diastolic pressures, cardiac output, or cardiac index over time.

This work focus on the validation of the *ClearSight System* device by analyzing the dynamics of the temporal series of continuously acquired signals. The objective was to characterize the synchronized signal obtained from 14 cardiac surgery patients. The BP data was collect for each subject with both invasive and non-invasive techniques. Both time series are compared using linear, time and frequency domain, and non-linear methods, such as entropy and compression. The correlation of the obtained measures with risk scores was also probed.

Differences were found between the signals collected by the two methods for all the studied indices. However, many of the parameters exhibited moderate to high correlations. The results obtained demonstrate that the Nexfin® device captures the dynamics of the BP signals. Furthermore, the signals acquired by the non-invasive method are related to the risk values. In particular, the entropy measures are inversely related to the Society of Thoracic Surgeons morbidity and mortality risk score, and the compression measures are inversely associated with the time spent in the intensive care unit.

The results suggest that the data collected by the Nexfin® device of the *ClearSight System* preserves the linear and non-linear data dimensions and that these data are correlated with the patients' cardiovascular risk assessment.

Acknowledgements

Firstly, I would like to thank Professor Teresa Henriques, my supervisor, for all the guidance throughout this work and for being so understanding and encouraging. It was a pleasure to work with you.

Afterward, I want to leave a thank you note to all my teachers who, during the last 17 years, have led me to my path and to discover my own passions.

Then, I want to thank my parents, my grandmother, and my sister Beatriz for their continuous support and for providing me everything I need to succeed in the future. Also, to the rest of my family, and my godparents who time after time embrace my achievements. A special thanks to my cousins Ana, David, and Nicolas for always trying to teach me through their own experiences.

Finally, I want to thank my friends.

To my all-time girlfriends Diana, Martins, and Sara for being always there, and, particularly, to Bá for this unique and amazing 21-year friendship and for being the person I can always count on. To Tiago, Branco, and Luís for all the times we lived together. To Francisca Albuquerque for being a more than wonderful friend since 2003.

And this 5-year experience would have not been the same without the friends that came out of it. To Leonor for being everything: a twin, a friend, a roommate, a travel buddy, my Erasmus partner, and the one who always understands me. To Pedro for driving me crazy every day but also for being always there for me and knowing me like anyone else. To Pedrão, Migas, Meneses, Gu, Álvaro, Ana, Bruno, Joana, Natalyia with whom I made (and will continue making) the best memories. To Francisca Agante and Francisca Ferreira that had also been a part of this adventure.

And finally, to the friends I made during my exchange semester in The Netherlands, especially, Charlotte D., Charlotte B., Mireia, Eva, Belisa, Mònica and Katelynn, with whom I lived the most wonderful time.

If the best is not yet to come at least it was amazing.

Raquel Pires Alves

"This morning I still have a lot of work to do,
I see that it isn't easy and will no doubt become much more difficult,
yet have unfaltering hope that I'll succeed,
and I'm also convinced that I'll learn to work by working,
and that my work will become better and more substantial."

Vicent Van Gogh

Contents

List of Figures

List of Tables

Abbreviations

ABP	Arterial Blood Pressure
ApEn	Approximate Entropy
BP	Blood Pressure
BPV	Blood Pressure Variability
CAB	Coronay Artery Bypass
CI	Cardiac Index
CNAP	Continuous Non-Invasive Arterial Pressure
CO	Cardiac Output
DBP	Diastolic Blood Pressure
ECG	Electrocardiogram
EP	Emergency Physician
EuroSCORE	European System for Cardiac Operative Risk Evaluation
FFT	Fast Fourier Transform
HF	High Frequency
HR	Heart-Rate
IABP	Invasive Arterial Blood Pressure
ICU	Intensive Care Unit
LF	Low Frequency
MAP	Mean Arterial Pressure
MF	Mid-Frequency
MSC	Multiscale Compression
MSE	Multiscale Entropy
NIBP	Non-invasive Intermittent Method
PAC	Pulmonary Arterial Catheterization
PiCCO	Pulse Contour Cardiac Output Monitoring
SampEn	Sample Entropy
SBP	Systolic Blood Pressure
SSR	Sum of Squared Residuals
STD	Standard Deviation
STS	Society of Thoracic Surgeons
SV	Stroke Volume
SVR	Systemic Vascular Resistance

Chapter 1

Introduction

1.1 Motivation and context

Blood pressure (BP) is one of the most important physiological signals with high clinical relevance. Its information can help the diagnosis of several diseases by giving valuable information on the heart condition, including blood vessels' walls thickness or clogging and pumping strength [1, 2].

Several methods can be used to assess the blood pressure, whether invasive or non-invasive and provide continuous or intermittent results [3].

In perioperative periods, the gold-standard method for measuring the BP is done by the placement of an intra-arterial catheter by a skilled clinician. This invasive procedure is associated with a risk of complications, including bleeding, infection, or ischemia. There is also proneness to measurement error as a result of the position variability within the vessel, perturbations in blood flow, and the frequency response of the transducer and ampifier [4].

Several devices that combine a non-invasive method with a continuous data collection are being developed to overcome the problems that can appear with the invasive procedure. However, to include these new methods in the actual clinical routines, the accuracy of the data must be verified as well as within patient's precision.

One of these devices that uses the volume clamp method to continuously measure the BP and a physical principle for initial and constant calibration is the *ClearSight System*. *ClearSight* is a system with an inflatable finger cuff that incorporates a Nexfin® device and measures cardiac output (CO) continuously with a light-absorption sensor by combining continuous BP monitoring with a novel pulse contour method. The Nexfin® device measures different parameters including continuous systolic BP (SBP), diastolic BP (DBP) and mean arterial BP (MAP) [5].

Several studies have been conducted to validate the usability of this non-invasive method (the Nexfin® device) by comparing it with invasive methods [6, 7, 8, 9, 10, 11]. The comparisons are based on the variation of isolated values such as MAP, systolic and diastolic pressures, CO, or cardiac index (CI) over time.

1.2 Goals

The goal of this work is to validate the BP data from the *ClearSight System* device by comparing the collected data signals to the gold-standard signals, invasively recorded. For that, several parameters will be collected from signals of both methods and compared. This will be done by analysing the dynamic of the temporal series, using frequency, variability, statistical and complexity measures, in order to establish a comparison based on the whole continuous signal. Subsequently, the relationship between those parameters and three different outputs: the Society of Thoracic Surgeons (STS) risk of mortality, the European system for cardiac operative risk evaluation (EUROScore) and the patient's time in the intensive care unit (ICU), will be studied.

Several tasks were outlined to asses these goals. The first one consists on the synchronization of the signals collected with the ClearSight System and the pulmonary arterial catheterization (PAC) method, Afterward, the selected linear and non-linear methods will be applied to the selected and pre-processed data. Third, the results obtained for the types of signals will be compared. Finally, in the fourth task, the risk indices information is going to be used to establish a relation between the used method and the obtained results to extract some conclusions.

Having this in mind, this work prospects in finding a new approach to validate the pertinence of the *ClearSight System* data in a preoperative setting.

1.3 Dissertation Structure

This work was divided into seven more chapters besides this introductory one.

Initially, Chapter 2 presentes relevant information on blood pressure, its variability, the measurement techniques, and values that can be recorded, and also how they can be related to different outcomes.

Chapter 3 explains, in detail, the *ClearSight System* and the Nexfin® device, its applications, and underlying technology, as well as the validation studies performed so far.

Chapter 4 shows the different signal processing techniques described, as well as the practical procedure used.

Chapter 5 presents the pre-processing mechanism and how the signals were treated before applying the techniques described in the previous chapter.

Afterward, Chapter 6 presents the results obtained for the different work phases and a brief description of them.

In Chapter 7, the results are discussed. Also, it is described the limitations faced throughout this work and how it can be improved in the future.

Finally, Chapter 8 presents the conclusions of the work developed under the scope of this dissertation.

Chapter 2

Blood pressure

2.1 Introduction

BP is expressed in systolic blood pressure (SBP) and diastolic blood pressure (DBP). SBP is the highest value of pressure during one heart cycle which corresponds to the heart muscle contraction. On the other hand, DBP is the lowest value of pressure between two heartbeats, which corresponds to when the heart chambers are being filled with blood [12]. The mean arterial blood pressure (MAP) is the average BP in an individual during a single cardiac cycle. It can also be described in function of the SBP and the DBP, as seen in equation[1] 2.1.

$$MAP = \frac{1}{3}(SBP - DBP) + DBP \tag{2.1}$$

When the measures of both SBP and DBP are higher than usual a patient is diagnosed with hypertension. The normal and hypertensive values of SBP and DBP are registered in Table 2.1.

			Hypertension	
	Normal Average	**Elevated**	**Stage 1**	**Stage 2**
SBP	120mmHg	120-129mmHg	130-139mmHg	+140mmHg
DBP	80mmHg	-	80-89mmHg	+90mmHg

Table 2.1: Range of systolic blood pressure (SBP) and diastolic blood pressure (DBP) values: normal, elevated and in hypertension cases [13]

Higher blood pressures and hypertension are associated with a higher incidence of complications and diseases such as coronary heart disease, stroke, and all cardiovascular diseases [14]. They also represent a major risk factor for cardiovascular morbidity, chronic kidney disease, and death [15].

[1] https://www.nursingcenter.com/ncblog/december-2011/calculating-the-map (last accessed Feb 2020)

Furthermore, a sudden elevation of the arterial BP (SBP or DBP), called a hypertensive emergency, can be related to life-threatening symptoms and spontaneous deaths. A patient with a hypertensive emergency should be hospitalized with continuous and thorough BP measuring [16].

Studies have found that SBP was more strongly associated with coronary heart disease death when compared to DBP, and isolated SBP elevation was found to be an important risk factor [17].

Moreover, there is evidence that treatments performed under local or general anesthesia may stress the cardiovascular system and, in general, increase the BP [18].

Despite these BP-triggering situations, it is important to know that BP is not constant throughout the day and, even if low, its variations can also infer about the patient's health [19]. Some reports have demonstrated that excessive fluctuations in BP values can be linked to early stages of myocardial, vascular, and renal organs damages [20] and other increases in mortality and cardiovascular events [21].

2.2 Blood pressure variability

As mentioned above, BP is not constant; it can change during several activities in response to autonomic, humoral, mechanical, myogenic, and environmental stimuli and, in a way, unique to each person [19, 22, 23].

BP can be characterized by its short-term fluctuations that occur within a 24h period (beat-to-beat, minute-to-minute, hour-to-hour, and day-to-night changes) and also long-term fluctuations occurring over more extended periods (days, weeks, months, seasons or years) [24]. The short-term variations can result from changes in heart-rate (HR), stroke volume, and systemic vascular resistance (concepts that are going to be explored further on) in response to external and internal stimuli [22].

Long-term fluctuations in BP occur when the baroreflex system, the homeostatic system responsible for maintaining the BP nearly constant, is unable to induce the feedback mechanisms that act on the HR and cardiac output to restore stability [25].

The Mayer waves are a representation of the variability noticeable in the BP signal and in the electrocardiogram (ECG). The waves appear in frequencies around 0.1Hz and can be a result of the feedback of several systems, such as the baroreceptor, chemoreceptor and centrogenic feedback systems [26]. Throughout the years, the shift of the Mayer wave frequencies to lower values is being linked to the increased risk of cardiovascular diseases [27].

Even though, in general, the adverse cardiovascular consequences of BP abnormalities largely depend on absolute BP values (MAP, DBP, and SBP), these outcomes might also depend on elevated and recurrent BP variability (BPV) [24].

Several studies report that enhanced fluctuation of BP confer cardiovascular risk and can induce left ventricular hypertrophy, vascular stiffness, and renal lesion [21, 22]. Both short-term and long-term BP excessive variability independently contributes to target organ damage (TOD), cardiovascular events, and mortality not only in hypertensive patients but also in subjects with *diabetes mellitus* and chronic kidney disease [21, 28].

In 2006, Young et al. [29] confirmed that the severity of hypertension is more closely related to a 24h mean BP than to single BP values. They also provide the first unequivocal demonstration that TOD is also connected to BP variability. This information reveals its utmost importance on the use of ambulatory BP measurement techniques to support the diagnosis of several conditions, including hypertension.

Furthermore, the study by Young et al. mentioned a cardiac metabolic gene that exhibits a circadian variation[2] by anticipating the changes in myocardial workload, synchronizing the substrate availability accordingly [29].

Considering that high BPVs strike a relevant cardiovascular risk factor [19], it is considered that the antihypertensive treatment should not only target reducing mean BP levels but also to stabilizing BPV to achieve consistent BP control over time [24]. In 2013, Hocht et al. stated that calcium channel blockers appear to be more effective than other BP lowering drugs for the reduction of short-term and long-term BPVs [21].

2.3 Blood pressure measuring

Monitoring the hemodynamic activity is a mainstay not only of critically ill patients but also as a routine analysis to detect heart-related diseases or malfunctions that can also impair the function of vital organs, such as the brain, heart, and kidneys [3].

The techniques used vary on the application and state of the patient and can be divided in non-invasive and invasive. The non-invasive methods can use intermittent and continuous techniques to measure the BP. All invasive methods provide continuous measures.

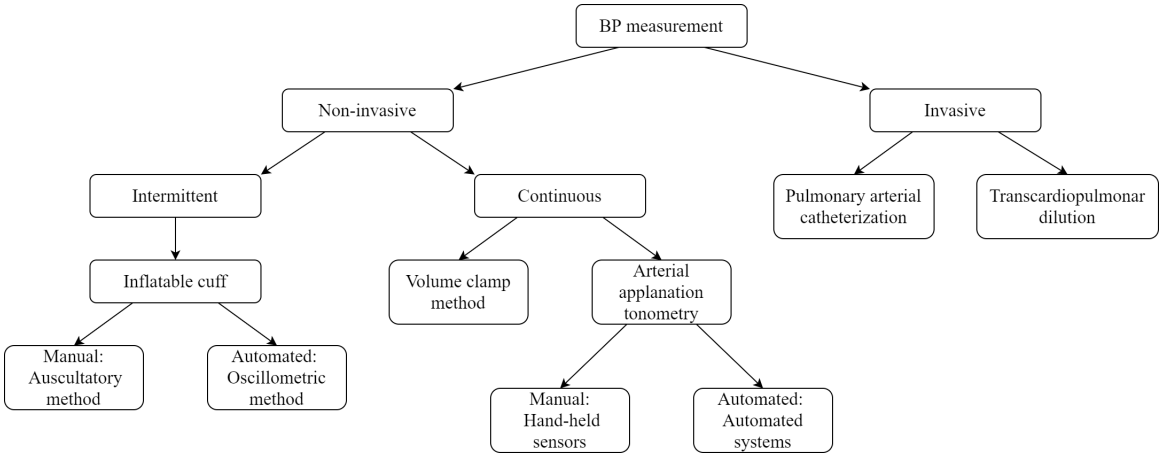

Figure 2.1: Diagram with the blood pressure monitoring techniques

The non-invasive intermittent measures are done with an inflatable cuff recurring to a stethoscope - manual or clinical method - or with the oscillometric approach - automated or ambulatory method. The non-invasive continuous methods can use either the volume clamp method or the arterial applanation tonometry (manual or automated). Finally, the invasive methods are the

[2] Variation according the sleep-wake cycle.

pulmonary arterial catheterization (PAC) and the transcardiopulmonar dilution. The diagram in Figure 2.1 has the distribution of these techniques.

2.3.1 Non-invasive intermittent BP measuring

BP has been traditionally measured in the clinical setting. However, recent technology improvements made it possible to be measured at home or in an ambulatory environment with high accuracy, improving the ability to evaluate the risk for target organ damage and hypertension related morbidity and mortality [30].

The clinical (manual) and the ambulatory (automated) measures of BP are done using an inflatable cuff tied around the patient's arm that is inflated occluding a major artery. When the pressure in the cuff slowly decreases, blood will begin to flow through the artery causing characteristic sounds - Korotkoff sounds - and the pressure in the cuff when blood first starts to flow continuously is an estimate of diastolic pressure [31]. The onset of the sounds corresponds to the patients' SBP, and the last sound at decreasing cuff pressure equals the patients' DBP [3].

The clinical measure of BP is done using a stethoscope and a mercury sphygmomanometer. In this method and during the cuff's deflation, the clinical practitioner uses a stethoscope to note the circulation sounds and the manometer display to make the correspondence between sound and pressure.

Conventionally, this procedure is done by a trained professional and, to avoid measurement errors, the cuff should have an appropriate size, the patient should be correctly positioned, rested, and should avert extraneous factors that influence blood pressure such as smoking and caffeine intake prior to the measurement [30].

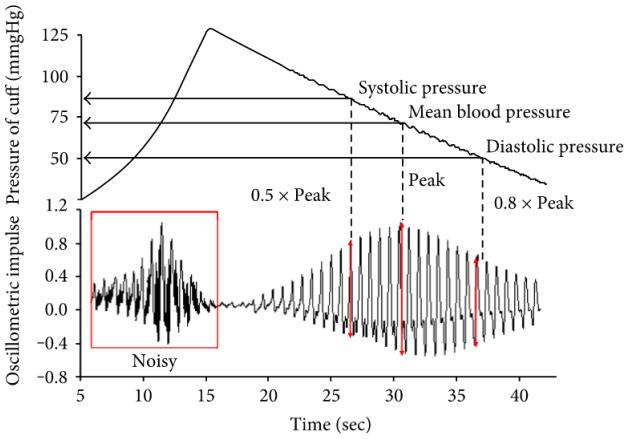

Figure 2.2: Cuff pressure waveform of oscillometric method [32]

The SBP can be estimated without the use of a stethoscope by feeling the radial pulse when the cuff is being deflated. This technique is not commonly used and also requires a quiet environment.

The ambulatory/automated measure of the BP uses the oscillometric method that establishes a correspondence between the pressure oscillations registered during the cuff's deflation and the BP. The mean BP corresponds to the highest peak on the oscillometric wave [33], and the DBP

and SBP are respectively, the pressure values for the 50% and 80% of the peak value in the oscillometric wave [34, 32] as it can be seen on Figure 2.2.

The ambulatory measuring is used to measure the BP at regular intervals to reduce sudden BP elevations or the white coat hypertension [3]. It requires the use of fully automated oscillometric devices that have been developed throughout the years [35]. Usually, these can be found in the form of a small cuff with an automated inflatable mechanism and an electronic equipment with a display screen, avoiding the problem of mercury toxicity related to the use of a mercury sphygmomanometer. They use the oscillometric method incorporated in a software that provides measures of SBP, DBP, and HR with high accuracy.

2.3.2 Non-invasive continuous BP measuring

Non-invasive continuous BP measuring techniques are the most recent ones and least used since their clinical validation still has not provided the expected and wanted results. These measurements can be based on two different techniques: the arterial applanation tonometry or the volume clamp method.

The arterial applanation tonometry is a technique based on the work of Pressman and Newgard [36]. They found that a transducer strapped to an artery with a bone underneath can obtain the arterial pulse wave. The technique can estimate the mean arterial pressure and allows the calculation of the SBP and DBP.

The pulse wave obtained by applanation tonometry contains more information than the SBP and DBP values. However, and despite being considered continuous BP measure techniques, these devices are made for a single timed interval analysis as they have to be handheld by the examiner. One of the devices that uses the automated radial artery applanation tonometry is the T-Line system, represented in Figure 2.3. This system has been evaluated in various clinical settings.

Figure 2.3: T-Line system device for applanation tonometry [37].

The second technique for non-invasive continuous BP measurement is the volume clamp method (or vascular unloading technology) based on the work done by Penáz [38].

[3] Effect that nervousness and anxiety caused by the clinical setting has on the patient's vital signs.

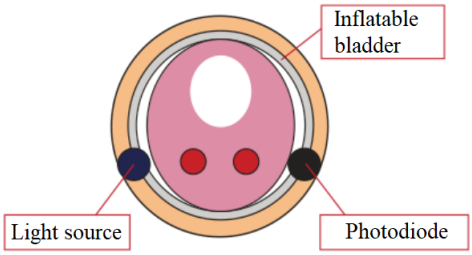

Figure 2.4: Representation of a plethysmograph used in the volume clamp methods[4]

The BP is measured with an inflatable cuff combined with a light source and photodiode placed at the finger. Figure 2.4 contains a representation of the setup. The plethysmograph uses the photodiode's information to measure changes in volume so that the pressure of the cuff can be adjusted to keep the artery's diameter constant. This is done by keeping the pressure in the cuff at the exact point where the finger does not show any more pulsations and there is no tension of the arterial wall. The pressure in the cuff follows the instantaneous value of intra-arterial BP. Afterward, with its changes, it is possible to create a BP curve that can be correlated to brachial artery BP through a reconstruction algorithm.

The devices in the market that are based on this technique are the *ClearSight System*[4] (Edwards, Irvine, CA, USA) and the CNAP® monitor[5] (CNSystems Medizintechnik AG, Graz, Austria), shown in Figure 2.5. The former will be described in detail in the next chapter.

Figure 2.5: Non-invasive continuous blood pressure measuring techniques: *ClearSight System*[4] (left) and CNAP® monitor[5] (right).

Both this methods measure the BP, HR, hemodynamics and fluid status, however, their bigger differentiation comes in the calibration method. The *ClearSight System* uses the Physiocal® method for initial and frequent calibration, whereas, the CNAP® monitor provides manual calibration, where the BP is measured externally and then the value is inserted in the system, or automatic calibration that uses an upper arm cuff to register the initial BP values.

These continuous non-invasive methods to monitor the BP are sensitive to the movement of

[4] https://www.edwards.com/gb/devices/Hemodynamic-Monitoring/clearsight (last accessed Feb 2020)

[5] https://www.cnsystems.com/products/cnap-monitor-500 (last accessed Feb 2020)

the patient, meaning that the values obtained for conscious individuals must be checked for plausibility. Furthermore, in the case of severe vasoconstriction, peripheral vascular disease, or distorted fingers due to arthritis, it might be difficult for the devices to obtain valid values and waveforms.

2.3.3 Invasive BP measuring

As a counterpoint to the non-invasive methods, there are the PAC and the transcardiopulmonar dilution methods. Both provide continuous hemodynamic measurements (beat to beat, including during the night)[39]. A study done in 2012 demonstrated that continuous measurement of BP detected hypotensive phases in 39% of the cases, whereas only 9% were detected using an intermittent method [40]. The invasive BP monitoring is usually indicated in the case of high-risk patients or complex surgical procedures. Most anesthesiologists recommend BP monitoring at least once every 5min in anesthetized patients undergoing surgical procedures [41].

The PAC consists of the insertion of a catheter into a pulmonary artery and is considered the standard for assessing CO, stroke volume (SV), systemic vascular resistance (SVR), and calculation of oxygen transport parameters in recent years [42]. The *Swan Ganz* catheter with an inflatable balloon at the tip that facilitates its placement into the pulmonary artery is the most commonly used one. This procedure, despite simple, requires some training and experience to avoid complications [43]. A study revealed that the incidence of *Swan-Ganz* catheter-associated pulmonary artery rupture is 0.031% [44].

The transcardiopulmonar thermal indicator dilution [42] is a method that uses a cold drug and a specific thermodilution arterial catheter (Pulse Contour Cardiac Output Monitoring, PiCCO) that measures temperature changes following the injection of the drug through a central vein catheter [45]. In some cases, the drug can be combined with a dye whose concentration is followed through time.

The setup required for these invasive methods is displayed in Figure 2.6. The transducer receives the reference pressure through the pressure bag containing a saline solution at 30mmHg. The transducer then converts the BP variations, captured through the catheter, into a digital signal that is amplified and displayed in the monitor [6].

These invasive procedures are associated with an increased risk of complications resulting in catheter placement which may include bleeding, infection, or ischemia. In addition, the measurement can suffer variations as a result of the position variability of the catheter within the vessel, perturbations in blood flow, and the frequency response of the transducer and amplifier [4]. To avoid the invasive procedure but still provide a continuous BP measure, numerous devices are being developed in the last years. The bigger challenge still resides in the accuracy of the data collected.

[6] http://www.memscap.com/applications-and-market-segments/medical-and-biomedical/invasive-blood-pressure (last accessed Jun 2020)

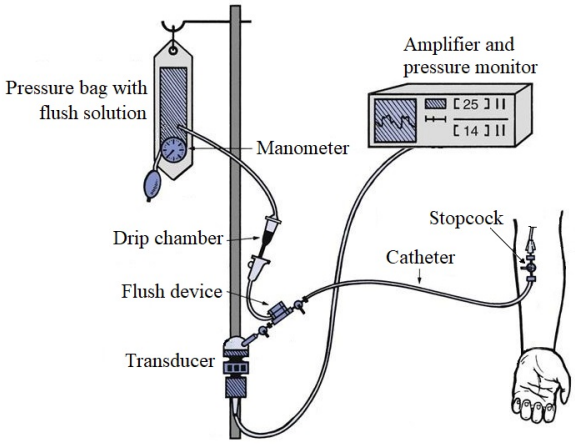

Figure 2.6: Pulmonary arterial catheterization setup.

2.4 Outcomes: Risk scores

The Society of Thoracic Surgeons (STS) Short-Term Risk and the EuroSCORE (European system for cardiac operative risk evaluation) are two indices that provide the risk of mortality and morbidities for a patient undergoing cardiac surgeries. They allow the identification of high-risk or "inoperable" patients [46]. These models serve as a statistical tool to account for the impact of a certain procedure on the patient's overall health[7] [47]. However, the STS morbidity and mortality risk score can only be calculated for patients undergoing certain types of surgery such as coronay artery bypass (CAB)[8], aortic and mitral valve procures.

Some studies reveal that the predictive power of the EuroSCORE is excellent, but usually, mortality is considerably overestimated by this score [48]. The mean EuroSCORE values are, in general, three times higher than the mean STS score values, and there is a reasonable linear relationship between them [46].

In addition, despite not being a risk score, the time a patient spends in ICU can be an indicator of his health state and his reaction to the surgery. Therefore, it can also be used as a parameter to assess the overall surgery risk and recovery.

[7] https://www.sts.org/resources/risk-calculator (last accessed Feb 2020)

[8] CAB is a surgical procedure done to restore the normal blood flow in an obstructed coronary artery, by grafting specific blood vessels

Chapter 3

ClearSight System

3.1 *ClearSight System* and Nexfin®

The volume clamp method - the finger cuff technology - allows for blood pressure to be measured non-invasively and continuously [49]. Devices such as the *ClearSight System* and the CNAP monitor that use this technology have been clinically tested, validated, and used in various settings [49, 50, 51]. Several tests made confirmed that these systems had the ability to track changes in blood pressure adequately, but the accuracy and precision of the data raised some concerns.

3.1.1 Application

The *ClearSight System* is indicated for patients going through moderated-risk surgeries that can not have an arterial catheter placed (arterial line) or whose use is not recommended. This system allows the monitoring of the different hemodynamic parameters [5], including the SV and SV variation, the CO, the SVR, the continuous BP. The system also gives valuable hemodynamic insight in moderate to high-risk surgery[1].

The *ClearSight System* incorporates the Nexfin® (BMEYE, Edwards, USA) monitor that provides the continuous BP waveform as well as the values of SBP, DBP, MAP, HR, and interbeat interval[2]. The EV1000 clinical platform, incorporated in the monitor, allows the visualization of the chosen parameters in a multi-option screen[1].

3.1.2 Underlying technology

As mentioned before, this technology is based on two methods: the volume clamp method to continuously measure BP [52] and the Physiocal® method for initial and frequent calibration [53].

[1] https://www.edwards.com/gb/devices/Hemodynamic-Monitoring/EV1000 (last accessed Feb 2020)

[2] https://medaval.ie/device/bmeye-nexfin/ (last accessed Feb 2020)

The volume clamp method involves clamping the artery providing equally distributed pressure on the arterial walls so that the volume of blood circulating in the artery remains constant. The volume is measured by a photo-plethysmograph built into the cuff, and the pressure is regulated upon these values [53]. This adjustment is made 1000 times per second.

Physiocal® is the real-time method to determine the arterial volume, considering the absence of a pressure gradient across the arterial wall. This method analyzes the curvature and sharpness of the plethysmogram and recalibrates the system automatically and periodically, allowing accurate tracking of physiologic variations [53, 6]. The Nexfin® monitor performs a brachial artery BP reconstruction since the finger arterial pressures usually differ physiologically from more proximal sites due to the narrowing of the arteries. That may result in more peaked wave shapes as well as decreasing mean BP. These effects are compensated using physiologic models [54], and that is the main difference in this technology when compared to previous products in the market, such as the Finapres® [55].

3.2 Validation studies

The introduction in the market of the Nexfin® Monitor with the CO-trek to monitor BP and CO occurred in 2007. Later in 2014, with the incorporation of the EV100 clinical platform, the *ClearSight System* entered the market[3]. This way, between 2009 and 2012, several studies were performed to validate the results obtained with the Nexfin® Monitor.

Regarding the comparison between the Nexfin® BP measurements and the BP obtained with a non-invasive intermittent method (NIBP), there are three works published.

The study done by Nowak et al. [56] in 2012 involved 40 emergency patients that had their CO and SVR estimated by an emergency physician (EP) and measured by the Nexfin® monitor in a baseline and after 2 hours of emergency assessment and treatment. This study stated that the values of CO and SVR estimated by the EPs and measured with the Nexfin® varied significantly, having an approximate agreement rate of 50%. In general, the EPs underestimated the seriousness of the results. The inability of EPs to accurately estimate these values was also reported with PAC measures - the gold standard, presenting similar results. It was concluded that the clinical assessment of hemodynamics depended on the treating doctor and are not accurate. This way, the use of a technology like the Nexfin® can provide objective and reliable results to assess CO and SVR.

In 2009, Akkermans et al. presented a study [57] where the values of SBP and DBP measured in 33 volunteers with a mercury sphygmomanometer were compared with the ones measured with the Nexfin® device. The Nexfin® passed phases 1 and 2.1 of the validation procedure of the European Society of Hypertension but did not pass phase 2.2 that is related to the variations within-subject. The European Society of Hypertension requirements for each phase are described

[3] https://www.edwards.com/gb/devices/Hemodynamic-Monitoring/clearsight (last accessed Feb 2020)

in Appendix A. Despite not meeting all the consitions, the study concluded that the Nexfin® device could be of value in a research setting or as a clinical BP monitoring system.

Eeftinck et al. presented a study in 2009 [55] where the Nexfin® device was compared with auscultatory BP measurements of 104 subjects. The differences (median and quartiles) between the two measurement methods were 5.4 (–1.7, 11.0) mmHg and –2.5 (–7.6, 2.3) mmHg for systolic and diastolic BP, respectively. They concluded that the Nexfin® device provided accurate results with good within-subject precision.

Several studies also compared the Nexfin® device with the gold standard for continuous BP measures - the PAC method.

In 2012, Martina et al. published a paper [6] where the two methods were compared in cardiothoracic surgery patients for 30 minutes. The results revealed that the correlation coefficients were 0.96 for SBP, 0.93 for DBP, 0.96 for MAP, and 0.94 for pulse pressure. The study concluded that BP could be measured non-invasively and continuously using the physiologic pressure reconstruction present in the Nexfin®. The values and their changes and variations are comparable to the ones obtained with PAC.

Also, in 2012 Fischer et al. developed a study [9] where SBP, DBP, MAP, and CI obtained from PAC, PiCCO, and the Nexfin® were compared. Six (12%) patients were excluded from the study because a reliable photoplethysmographic signal could not be obtained, revealing an important pitfall of the Nexfin® device. For the other 44 patients, there was a significant relationship between the photoplethysmographic and the PAC signal, with a correlation coefficient of 0.56 for SBP, 0.61 for DBP, and 0.77 for MAP. Between the PiCCO and the Nexfin®, device the correlation coefficient obtained for the CI was 0.33, corresponding to an error of 50%. They concluded that the Nexfin® device is reliable, safe, and convenient to measure BP, but it cannot be considered a way to replace PiCCO's measure of CI.

Kalmar et al., in 2012, also presented a study [8] with 110 patients that concluded that the the accuracy of the MAP obtained with the Nexfin® was higher than with the NIBP that does not provide a continuous measurement. In addition, the Nexfin® device was considered stable without requiring a long calibration time, providing satisfactory accuracy for most procedures.

Finally, Martina et al. have also published another paper [7] earlier, in 2010, where the Nexfin® device was compared with the PAC in patients with reduced arterial pulsatility. The average difference between the two methods was -1.3±6.5 mmHg. Therefore, it was concluded that the Nexfin® monitor enables clinicians to measure ABP waveform non-invasively supported by continuous-flow left ventricular assist devices without the risks related to invasive measurements.

Chapter 4

Signal processing techniques

4.1 Introduction

The signal obtained with the Nexfin® device is a digital signal with the BP information and its variations. In order to evaluate the signal and compare it with the invasive arterial BP (IABP), some features of the time series must be studied. The next sections will be destined to explain the different methods used to interpret and analyze the signal. These methods were divided into linear time and frequency domain methods and non-linear methods.

4.2 Time domain methods

A time-domain approach considers the signal as a sequence of an unordered set of intervals [58]. It acknowledges the signal as a discrete or continuous progression over time.

For the first two approaches, two of the parameters that can be calculated are the mean and the standard deviation (STD) (or variance). Considering a discrete signal acquired with a specific sampling rate, the mean (μ) and the standard deviation (δ) can be determined through equations 4.1 and 4.2, respectively [1]. The variance corresponds to the square of the standard deviation (δ^2).

$$\mu = \frac{1}{N}\sum_{i=0}^{N-1} x_i \tag{4.1}$$

$$\delta^2 = \frac{1}{N-1}\sum_{i=0}^{N-1} (x_i - \mu)^2 \tag{4.2}$$

Taking this into consideration, the first analysis done included the BP mean value and standard deviation for each patient, as well as, the difference between those values of the two methods

[1] https://www.statisticshowto.datasciencecentral.com/probability-and-statistics/correlation-coefficient-formula/ (last accessed Feb 2020)

and, also, the relative error. The relative error can be computed through equation 4.3, where x_0 corresponds to the value obtained with the Nexfin device and x is the value measured invasively.

$$E_r(\%) = \frac{x_0 - x}{x} \cdot 100 \tag{4.3}$$

4.3 Frequency domain methods: spectral analysis

The frequency-domain methods allow an interpretation of a signal as a function of frequencies instead of time. This approach gives information on the distribution of the signal within each frequency band over a range of frequencies. Spectral estimation methods compute the power as a function of frequency [59].

The transition from a signal in the time domain to the frequency domain can be calculated mathematically using the Fourier transform or its fast algorithm, the Fast Fourier Transform (FFT). The result of the FFT is a complex number for each frequency present in the signal data [60], and its spectrum is characterized by discrete peaks in each frequency component [61].

One of the analyses that can be done in the spectral domain is the partitioning of the signal in high and low-frequency variabilities (HFs and LFs) that gives information on the short-term or long-term variability of the time series [60]. The variability can be obtained by calculating the total area under the power spectral density curve [60].

The spectral components (frequency bands) are, in general, classified into four different power categories that can be distinguished in the calculated spectrum.

Regarding the blood pressure signals, the HF range lies within the 0.2, and the 0.4 Hz, the mid-frequency (MF) range lies around 0.1 Hz, and the LF range is within the 0.02 and 0.07 Hz [2]. The HFs are associated with a normal respiratory, activity whereas the MFs can be related to the Mayer Waves. The peaks width and length around these frequencies are not constant, but the control mechanism can be determined through the power or the area of the peaks in the wanted frequency range [63, 26].

In this work, it was computed the FFT and, afterward, it was determined the area of the spectrum in the HF region and the MF region. The MF interval was defined between 0.07 and 0.13Hz.

Another analysis that can be done when working in the frequency domain and when comparing two different signals is the coherence index. It comes up as a counterpoint to the correlation function used in the time domain [64]. It can be calculated using equation 4.4, where Gxy is the cross-spectral density between the two signals, and Gxx and Gyy are the autospectral density of each signal. The magnitude of the coherence function is an index of the relation between the two signals. These values were also collected for each signal type and patient.

$$C_{xy}(f) = \frac{|G_{xy}|^2}{G_{xx}G_{yy}} \tag{4.4}$$

[2] In some cases, the LF range is discarded and the MF range is named LF [62, 63]

4.4 Non-linear analyses

The non-linear analysis of a signal focuses on its distribution, analyzing its properties in interval sequences [58, 65].

Inside the non-linear measures that are currently used to characterize physiological signals, complexity measures are widely used to outline the amount of structured information. Complexity perceives irregularity, subjectivity, and uncertainty as a fundamental part of every system [66]. Furthermore, dynamical complexity can indicate the adaptability of the system to internal and external stimuli. This ability to adapt is higher in healthy organisms and decreases with elderliness and the presence of pathologies [4].

The complexity measures can be divided into entropy measures and compression measures. The application of compression algorithms on biological systems is still under development. However, some studies have demonstrated that it can be used as an alternative to the entropy and that the combination of both methods can quantify different features of a system's complexity, improving the characterization of different pathophysiological states [66].

4.4.1 Entropy measures

The first introduction of the entropy measure occurred in 1948 by Shannon [67], who attempted to determine how random a message is expected to be within a given distribution.

Considering X, a random variable with a distribution $P(X = x) = p_x$, the Shannon entropy of the random variable X is given by equation 4.5, and it is measured in bits [68].

$$H(X) = \sum_{x \in Y} p_x log_2 \frac{1}{p_x} \tag{4.5}$$

Later in 1991, the concept of approximate entropy (ApEn) appeared as a new way to classify complex systems [69]. For N given points of a time series x, ApEn(N,m,r) is calculated using equation 4.6 where $\Phi^m(r)$ and $C_i^m(r)$ are obtained through equations 4.7 and 4.8, respectively, where d is the distance between the vectors $x(i)$ and $x(j)$, given by the maximum difference between their corresponding scalar components. The parameters m (subseries length) and r (tolerance) can be variable depending on the context. A system with a low ApEn value is considered a system with a high degree of regularity [66, 69].

$$ApEn = \Phi^m(r) - \Phi^{m+1}(r) \tag{4.6}$$

$$\Phi^m(r) = (N-m+1)^{-1} \sum_{i=1}^{N-m+1} log(C_i^m(r)) \tag{4.7}$$

$$C_i^m(r) = \frac{\text{number of x(j) such that } d[x(i),x(j)] \leq r}{N-m+1} \tag{4.8}$$

In 2000, Richmann introduced the notion of sample entropy (SampEn) with to reduce the ApEn bias and provide an approach more suitable for biomedical signals [70]. SampEn(m,r) is

computed using equation 4.9, in which the parameters m and r allow the change of the size of segments used to help the detection of larger or smaller patterns.

$$SampEn(m,r) = -log\frac{\text{number of template vector pairs having } d[X_{m+1}(i),X_{m+1}(j)] < r}{\text{number of template vector pairs having } d[X_m(i),X_m(j)] < r} \quad (4.9)$$

For this work, the parameters chosen when determining both the ApEn and the SampEn for each signal were $m = 2$ and $r = 0.15 \times standard\ deviation$, following the proxy presented in the study by Gibson et al. in 2018 [4].

The SampEn was also used to assess the short-term fluctuations of the signals by comparing the SampEn value of the first differences of the original pre-processed signals with the value of the first differences of the surrogate signals. The first differences are the difference between consecutive values of the signal, and the surrogate is done by randomly shuffling the points in the signal. This process was done 100 times for each signal and, afterward, the mean SampEn value is the one registered. This procedure is important to determine whether the observed short-term fluctuations of the BP time series have some information or are random noise. Similar entropy values between the original and the surrogate signals indicate that there is no information in those fluctuations.

To provide an analysis of a physiological time series, Costa et al. proposed, in 2002, the multiscale entropy (MSE) technique, a function of the entropy per scale [71]. The MSE method measures the SampEn for a set of time series on different time scales [4]. The use of multiple measurements of entropy allows the assessment of complexity at shorter and longer time scales [72, 4].

For the multiscale entropy analysis, it was used the 5 scales, and, for each signal, it was computed the MSE_{slope}, the MSE_{Σ}, and the $MSE_{slope \cdot \Sigma}$. The MSE_{slope} is the linear regression slope between the 5 SampEn values, the MSE_{Σ} is considered the complexity index and is the sum of the 5 SampEn values and, finally, $MSE_{slope \cdot \Sigma}$ is the product between MSE_{slope} and MSE_{Σ}. It was used the same values of m and r as the ones used previously for the SampEn.

4.4.2 Compression measures

One of the approaches to measure the complexity of a signal is the Kolmogorov complexity [73]. However, its application in biomedical signals is limited by the fact that the Kolmogorov complexity is not computable. The compressors are a close upper-bounded approximation of the Kolmogorov complexity function.

The purpose of data compression is to encode information using fewer bits than the original data to save data memory.

The compressors can be divided into two main types: lossless and lossy compressors. The lossless compressors preserve every bit of data in the file after uncompression, whereas lossy compressors eliminate certain bits of information, especially redundant ones [66].

When it comes to measuring the complexity of a digital signal, several compressors can be used, being the Lempel-Ziv compressor[74] and the GZIP [75] the most commonly used and adopted in this work . The GZIP compressor was launched in July 1992 by Jean-Loup Gailly and Mark Adler[3] and the LZMA compressor (Lempel–Ziv–Markov chain algorithm) has been developed by Igor Pavlov since 1996 and uses the Burrows–Wheeler transform algorithm[4]. Both compressors perform lossless data compression with a high compression ratio.

In the multiscale compression (MSC) analysis, the BP signals were compressed using 5 different scales and the ratio (original/compressed) was calculated for each scale. Afterward, it was registered the scale 1 ratio, the slope (MSC_{slope}), and the sum (MSC_{Σ}) between the 5 scales ratios and also the product between the slope, and the sum ($MSC_{slope \cdot \Sigma}$).

4.5 Association with the outcomes

Demographic and clinical characteristics are summarized by their median, first and third quartiles in the case of continuous variables, and by count number and percentage in the case of categorical variables.

For the comparison of two signals obtained with different methods, a correlation coefficient gives information on the statistical relationship between both. It can be computed with equation 4.10, and it ranges from -1 to 1, where higher absolute values indicate a higher linear correlation between the two signals. It is important to mention that a high correlation does not mean that the two methods agree [76].

$$r = \frac{n(\sum xy) - (\sum x)(\sum y)}{\sqrt{[n\sum x^2 - (\sum x)^2][n\sum y^2 - (\sum y)^2]}} = \frac{cov(x,y)}{\sqrt{var(x) \cdot var(y)}} \tag{4.10}$$

This correlation coefficient is also known as the Pearson correlation coefficient to which can be associated with a p value that represents the significance level of the correlation [77, 78]. A high p value might be related to a random data relation, whereas, a low p value ensures the idea that the two data series are linearly related.

The Spearman correlation test is similar to the Pearson test but assesses if there is a monotonic relation between the two variables, even if not linear [79]. It also ranges from -1 to 1 where higher absolute values indicate the monotonic relationship. This correlation coefficient is considered to be the Pearson correlation coefficient for the rank variables and has also associated a p value to test its statistical relevance.

Furthermore, to test differences in the population's distribution, the Wilcoxon paired test was used [80].

These two methods, the Spearman correlation coefficient, and the Wilcoxon test, were applied to compare the indices derived from invasive versus noninvasive ABP time series.

[3] http://www.gzip.org (last accessed May 2020)

[4] https://en.wikipedia.org/wiki/Lempel%E2%80%93Ziv%E2%80%93Markov_chain_algorithm (last accessed May 2020)

One of the main goals of this work is to relate the different indices obtained from the previously described methods to the EUROScore, the STS, morbidity and mortality risk, and the ICU time. For that, a linear regression was performed. Similarly to what was done by Henriques et al. in 2019 [81], all three outcomes were logarithmically transformed to increase their linear relationship with the parameters and minimize the sum of the squared residuals (SSR).

In this procedure, the correlation coefficients were also standardized (divided by the standard error) so that they could be comparable.

Additionally, the linear regression performed for the ICU time also included information on the patients' age. That was not done for the risk scores considering their values already consider that parameter.

Statistical significance was set at p-values < 0.05. A sample of 14 paired observations provides 80% power to detect effect sizes of 0.89 (i.e., we are powered to detect differences between methods of 0.89 times the STD). This calculation allows for a 10% loss of efficiency for the non-parametric test (relative to the paired t-test).

Chapter 5

Signals pre-processing

Before applying the non-linear measures to the blood pressure time series, a signal pre-processing is required. In this chapter, we describe the data demographics and the pre-processing used. All the data pre-processing and analysis was done using the Python software.

5.1 Sample population analysis

In this work, it will be used blood pressure data from 14 adult patients (18 years. or older) collected from September to December 2017 with informed consent, as part of an ongoing prospective, single tertiary care center observational study funded by the National Institute of Health (R01GM098406). The Institutional Review approved the protocol Board of Beth Israel Deaconess Medical Center. All data were deidentified before analysis. The BP was obtained using both an invasive method, the PAC, and a non-invasive method - the Nexfin® of the *ClearSight System*.

Table 5.1: Patient's clinical characteristics and surgical data[1].

	All patients (n=14)	
Age (y), median (Q1, Q3)	70	(64.2, 79.5)
Gender (male), n (%)	13	(92.9%)
STS Mort+Morb (%), median (Q1, Q3)	9.8	(6.2, 10.5)
EuroSCORE index, median (Q1, Q3)	2.3	(1.0, 3.0)
Time in ICU (h), median (Q1, Q3)	29.1	(24.8, 45.0)
Surgery type:		
CAB, n (%)	10	(71.4%)
Valve, n (%)	5	(35.7%)
Other, n (%)	2	(14.3%)

Of the 14 patients, 13 were male, and 1 was female, with ages ranging from 48 to 84 years. The data was collected in a preoperative period where patients were mainly indicated for CAB or a valve replacement surgery. Seven patients were in an urgent state.

The patients' clinical characteristics and surgical data are present in Table 5.1 and, Appendix B compiles the detailed information for each subject analyzed.

5.2 Signals representation

The data collected with the PAC and the Nexfin device of the *ClearSight System* for the 14 patients were grouped into different files. The invasive data was divided into MAP, DBP, SBP, and pulmonary arterial pressure, all values as a function of time and separated for each patient. For the non-invasive data, the values included the time, unreconstructed and reconstructed values of MAP, DBP, and SBP, and status data. Note that the reconstructed values of BP imply a certain degree of pre-processing that is not disclosed. For this work, it was only used the reconstructed dataset.

The values of SBP, DBP, and MAP for both methods were plotted, and, in Figure 5.1, those can be seen for one representative patient (patient 5).

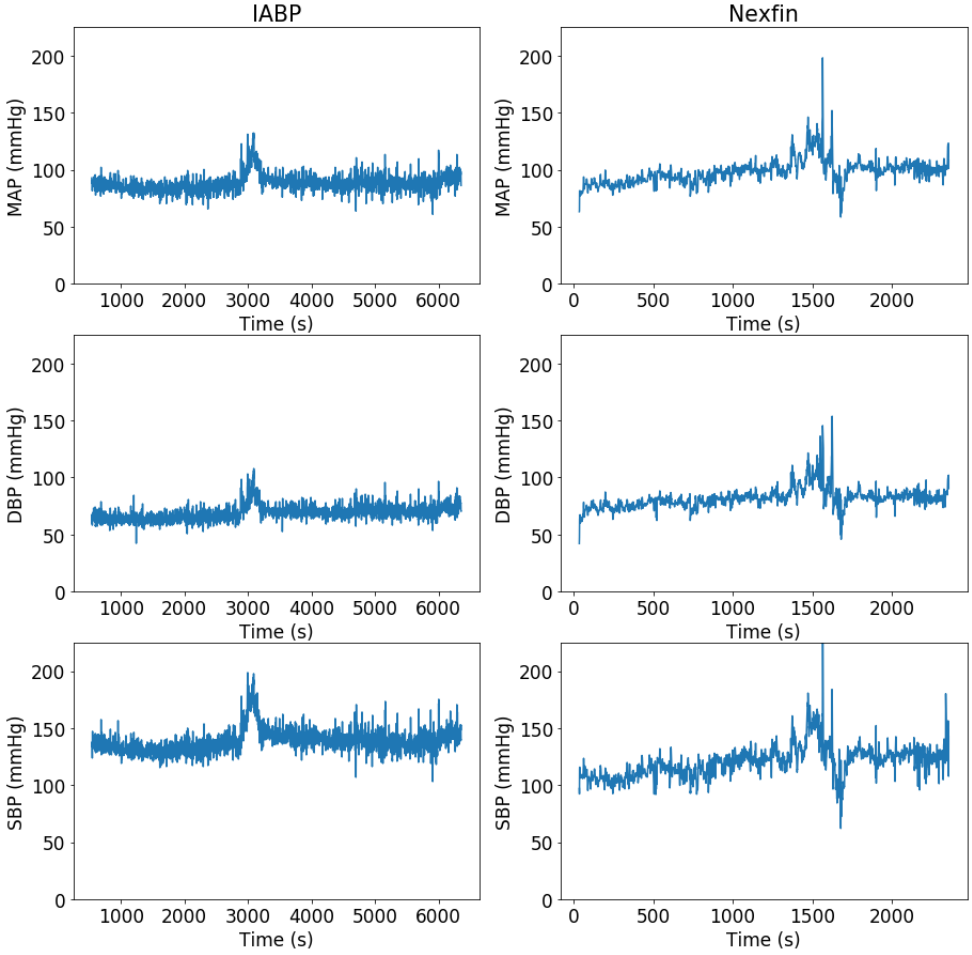

Figure 5.1: Representation of the raw signals obtained with the PAC and the Nexfin device of the *ClearSight System* for the MAP, DBP and SBP - example of the patient 5

These representations only allow for a simple comparison of the two methods, and, it can be seen, the two signals are not synchronized, and the length of the signals acquired with the non-invasive method is inferior to the ones obtained from the invasive method.

5.3 Data Synchronization

The signals require a synchronization that was initially done based on the time of the beginning and end of the signal acquisition. The synchronization was achieved by removing the points where the signals were not being simultaneously acquired.

Even though this automatic synchronization was not ideal, this process allowed the identification of patterns in both invasive and non-invasive signals that enabled the determination of adjustment needed for manual synchronization. Figure 5.2 compiles the plots of the signals for patient 5 after the automatic and manual synchronization. In this case, the manual adjustment was +73 seconds, where the positive value means that the Nexfin signal is delayed when compared to the IABP signal.

The adjustment made is dependent on the subject, and there was no pattern observed in it. Despite that, those values are presented in Appendix B.2.

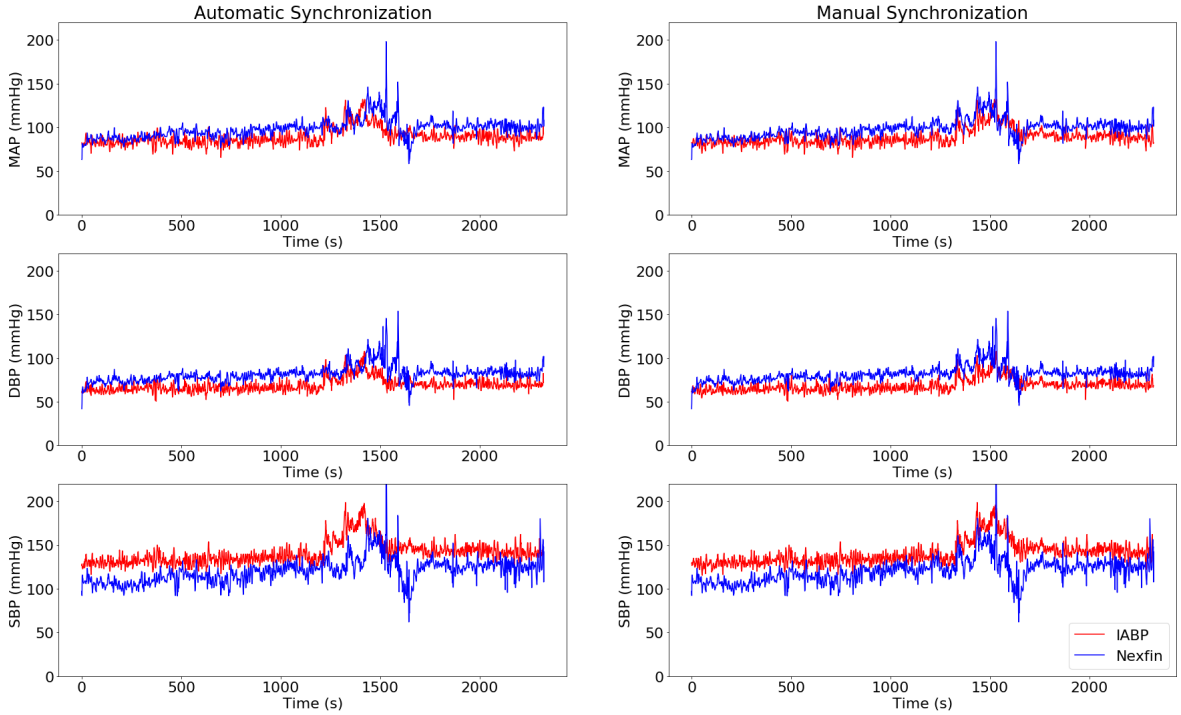

Figure 5.2: Representation of the signals of patient 5 after automatic synchronization.

5.4 Division into segments

Following the manual synchronization, it was done a division of each signal into different segments to normalize the length between the signals of the various patients. The segments were created so that they had around 700 points, ranging from 634 to 853, to maximize the number of segments and avoid the loss of information. Table B.3 in Appendix B contains the correspondence

between patient to segment and its respective length. In all, it was created a group of 33 segments for the 14 patients.

Chapter 6

Signal analysis

Several measures were applied to compare the invasive and non-invasive BP signals. The methods chosen and procedures were presented in Chapter 4 and include statistical measures, a complexity analysis through entropy and compression methods, and a frequency analysis. In addition, it was studied the relationship between these parameters and the different outputs through linear regression analysis. This chapter present the results obtained.

6.1 Time domain measures

Table 6.1 presents the mean, the standard deviation, the difference between these parameters of the two methods, and the relative error between means (Nexfin®-IABP) for each of the BP time series.

Table 6.1: Time domain measures of invasive arterial blood pressure versus noninvasive blood pressure (Nexfin®). P-values in bold are lower than 0.05.

	IABP (n=14) Median (Q1, Q3)	**Nexfin® (n=14) Median (Q1, Q3)**	**Difference (Nexfin® - IABP) Median (Q1, Q3)**	**Relative Error (%) Median (Q1, Q3)**	**Wilcoxon P**
Time series mean					
MAP	72.1 (67.5, 76.0)	95.0 (85.8, 101.5)	17.4 (15.5, 29.6)	26.3 (20.1, 46.9)	**<0.001**
DBP	50.1 (45.2, 56.8)	71.7 (64.9, 75.7)	18.8 (14.8, 26.2)	36.4 (28.6, 53.5)	**<0.001**
SBP	138.5 (123.9, 144.8)	131.2 (115.7, 151.0)	0.5 (-12.3, 7.0)	-0.3 (-9.7, 5.7)	0.826
Time series STD					
MAP	5.9 (4.9, 7.0)	7.9 (6.7, 9.0)	1.8 (0.5, 2.6)	30.0 (9.7, 50.2)	**0.004**
DBP	5.0 (4.2, 6.1)	6.0 (5.3, 7.7)	1.1 (0.7, 2.0)	22.4 (16.6, 33.7)	**<0.001**
SBP	7.8 (6.2, 9.1)	10.8 (8.6, 11.9)	2.6 (1.6, 3.5)	34.3 (16.4, 53.1)	**0.006**

Abbreviations: IABP, invasive arterial blood pressure; MAP, mean arterial blood pressure; DBP, diastolic blood pressure; SBP, systolic blood pressure; Q1, first quartile; Q3, third quartile; STD, standard deviation.

The mean BP values are significantly higher for DBP and MAP when acquired by Nexfin® comparing with the invasive ones. The STD of all the BP is higher in the signals obtained by Nexfin® than the invasive ones. The relative error of the mean is higher for the DBP and lower

for the SBP. As a counterpoint, the relative error of the standard deviation is higher for the SBP and lower for the DBP.

6.2 Frequency analysis

For the frequency analysis of the signals, it was fundamental that each signal had a constant sampling frequency. For that, signals were re-sampled by maintaining the same number of points and duration and by interpolating the unknown points. However, in this process, some information or noise can be lost, and signal peaks may appear less prominent. Figure 6.1 represents the original plot of a segment of patient 2 (segment 3) and the re-sampled version.

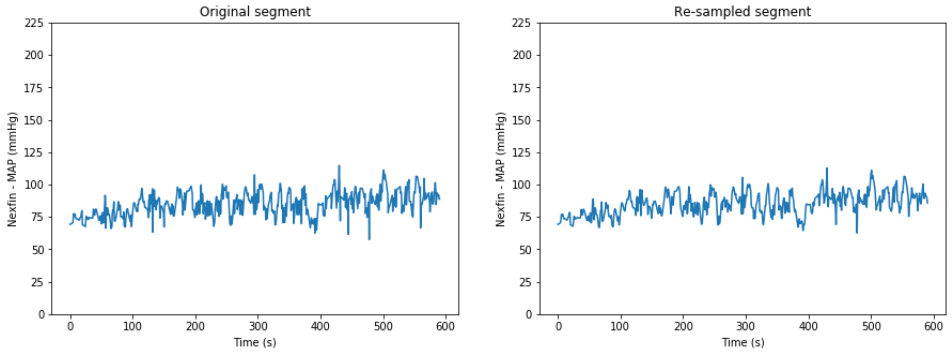

Figure 6.1: Original and re-sampled signals of the mean arterial blood pressure (MAP) of the Nexfin® device for a segment of patient 2.

After the signals were sampled, it was determined the area of the spectrum in the HF region and the MF region. Figure 6.2 represents the frequency spectrum for the MAP signal acquired with the Nexfin® device for the third segment, where it is possible to see the general aspect of the BP spectrum. The HF and MF area values are registered in Table 6.2, as well as the Spearman correlation parameters and the p-value of the Wilcoxon paired test.

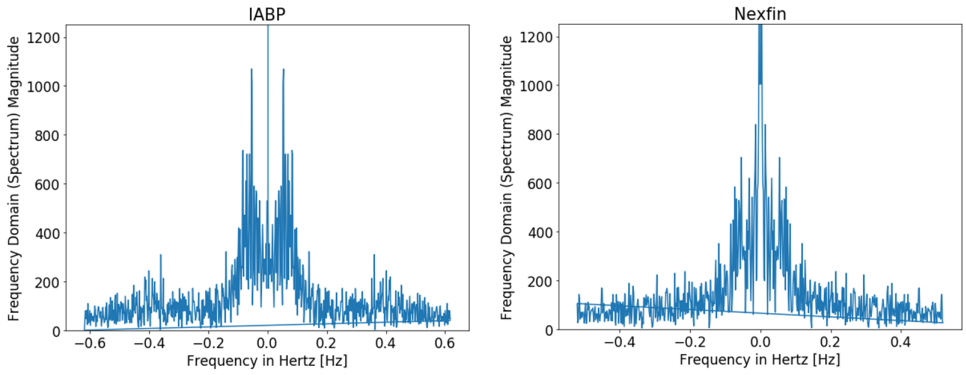

Figure 6.2: Spectrum of the mean arterial blood pressure (MAP) signals of the invasive method (left) and of the Nexfin® device (right) for a segment of patient 2.

The HF and the MF areas are significantly higher for the Nexfin® device for the MAP and SBP time series. The values of the HF area of the MAP and SBP signals and the MF area for the SBP for both types of acquisition are highly correlated.

Table 6.2: Area of the spectrum in high frequency and mid-frequency regions of invasive arterial blood pressure and noninvasive (Nexfin®) blood pressure signals. Spearman correlation and Wilcoxon paired test for the comparison of the two methods. P-values in bold are lower than 0.05

	IABP	**Nexfin®**	**Spearman**		**Wilcoxon**
	Median (Q1, Q3)	**Median (Q1, Q3)**	**r (95% CI)**	**P**	**P**
HF area					
MAP	1.48 (0.94, 1.99)	1.94 (1.30, 2.84)	0.93 (0.79, 0.98)	**<0.001**	**0.011**
DBP	1.22 (1.03, 1.42)	1.96 (0.72, 2.63)	0.28 (-0.29, 0.71)	0.326	0.177
SBP	1.99 (0.98, 2.68)	3.40 (2.06, 3.91)	0.64 (0.17, 0.88)	**0.013**	**0.003**
MF area					
MAP	1.42 (0.76, 1.75)	1.72 (1.16, 2.59)	0.47 (-0.08, 0.80)	0.088	**0.030**
DBP	1.04 (0.70, 1.44)	1.19 (0.96, 2.46)	0.36 (-0.21, 0.75)	0.203	0.096
SBP	1.35 (0.82, 2.46)	2.22 (1.73, 2.90)	0.71 (0.28, 0.90)	**0.005**	**0.016**

Abbreviations: IABP, invasive arterial blood pressure; MAP, mean arterial blood pressure; DBP, diastolic blood pressure; SBP, systolic blood pressure; HF, high- frequency; MF, mid-frequency; Q1, first quartile; Q3, third quartile.

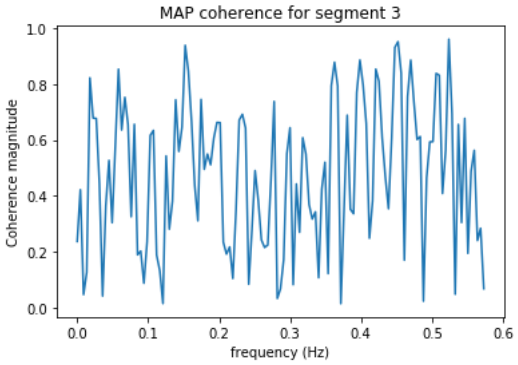

Figure 6.3: Coherence plot of the mean arterial blood pressure (MAP) signal of segment of patient 2.

Table 6.3: Coherence between invasive and non-invasive signals. It is presented the median and quartiles for the average coherence value of each patient's signal and for the entire spectrum, the HF range and the MF range.

	Median (Q1, Q3)		
	Entire spectrum	**HF range**	**MF range**
MAP	0.58 (0.56, 0.62)	0.51 (0.49, 0.54)	0.72 (0.71, 0.73)
DBP	0.51 (0.50, 0.54)	0.43 (0.43, 0.46)	0.65 (0.62, 0.67)
SBP	0.49 (0.49, 0.51)	0.42 (0.41, 0.45)	0.58 (0.58, 0.60)

Abbreviations: IABP, invasive arterial blood pressure; MAP, mean arterial blood pressure; DBP, diastolic blood pressure; SBP, systolic blood pressure; HF, high- frequency; MF, mid-frequency

Regarding the coherence analysis, it was computed the values for the entire spectrum and also for the HF and MF range. Figure 6.3 is a representation of the coherence function for the segment 3. The mean values for the entire spectrum range, and for the HF and MF ranges are presented in Table 6.3. The coherence value is higher for the MAP signal and, in general, the values are higher for the MF range.

6.3 Short-term fluctuations

The short-term fluctuations were measured through the comparison of the sample entropy of the first differences of the original pre-processed signals with the sample entropy of the first differences of the surrogate signals. The results are present in Table 6.4. The entropy values are significantly higher for the surrogate signals.

Table 6.4: Sample entropy for the first differences of the original and surrogate signals. It is presented the median, the first and third quartiles, the median of difference between the original and the surrogate and its quartiles and the Wilcoxon p-value. P-values in bold are lower than 0.05.

	Original Median (Q1, Q3)	**Surrogate Median (Q1, Q3)**	**Difference (Surrogate-Original)**	**Wilcoxon P**
Invasive ABP				
MAP	2.13 (1.87 - 2.33)	2.87 (2.64 - 2.98)	0.72 (0.31 - 1.05)	**0.002**
DBP	2.00 (1.54 - 2.10)	2.81 (2.68 - 2.91)	0.85 (0.48 - 1.28)	**0.002**
SBP	2.42 (2.13 - 2.65)	2.63 (2.55 - 3.08)	0.40 (-0.12 - 0.70)	**0.026**
Nexfin®				
MAP	2.10 (1.89 - 2.37)	2.62 (2.54 - 2.69)	0.43 (0.30 - 0.54)	**0.002**
DBP	2.04 (1.87 - 2.30)	2.50 (2.42 - 2.61)	0.47 (0.20 - 0.67)	**0.001**
SBP	2.12 (2.03 - 2.35)	2.58 (2.49 - 2.66)	0.40 (0.16 - 0.54)	**<0.001**

Abbreviations: IABP, invasive arterial blood pressure; MAP, mean arterial blood pressure; DBP, diastolic blood pressure; SBP, systolic blood pressure.

6.4 Entropy analysis

Regarding the entropy analysis, we first computed the sample entropy, and the Shannon entropy, where the values obtained are presented in Table 6.5.

The values obtained for the Shannon entropy are significantly higher for the Nexfin® signals. For the MAP and SBP signals, there is evidence of a strong correlation between the two methods. The same is not observed for the SBP. On the other hand, the SampEn values for the DBP time series did not show significant differences between the two acquisition methods. In this case, the Spearman coefficient shows a moderate correlation between the two methods only for the MAP signal.

The variations of the entropy for the 5 scales are displayed in Figure 6.4, where the values of the SampEn are closer in higher scales. Also, IABP's sample entropy is consistently higher than Nexfin®'s BP.

Table 6.5: Shannon Entropy and Sample Entropy for the mean arterial blood pressure, diastolic blood pressure, and systolic blood pressure registered with the invasive method and the Nexfin® device. It is presented the median, the first and third quartiles and the Spearman correlation coefficient (r) and p-value and the Wilcoxon paired test. P-values presented in bold are lower than 0.05.

	IABP	**Nexfin®**	**Spearman**		**Wilcoxon**
	Median (Q1, Q3)	**Median (Q1, Q3)**	**r (95% CI)**	**P**	**P**
Shannon Entropy					
MAP	4.5 (4.2, 4.7)	6.6 (6.4, 6.8)	0.72 (0.31, 0.91)	**0.003**	**<0.001**
DBP	4,1 (3.9, 4.4)	6.2 (6.1, 6.5)	0.82 (0.51, 0.94)	**<0.001**	**<0.001**
SBP	5.0 (4.7, 5.1)	7.0 (6.7, 7.1)	0.39 (-0.18, 0.76)	0.169	**<0.001**
Sample Entropy					
MAP	2.5 (2.3, 2.8)	2.3 (2.1, 2.4)	0.69 (0.26, 0.89)	**0.006**	**0.001**
DBP	2.3 (1.9, 2.4)	2.2 (2.1, 2.3)	0.51 (-0.03, 0.82)	0.061	0.925
SBP	2.7 (2.4, 2.9)	2.3 (2.2, 2.4)	0.12 (-0.44, 0.61)	0.692	**0.026**

Abbreviations: IABP, invasive arterial blood pressure; MAP, mean arterial blood pressure; DBP, diastolic blood pressure; SBP, systolic blood pressure; CI, confidence interval; Q1, first quartile; Q3, third quartile.

All three MSE metrics obtained are presented in Table 6.6. The MSE_{slope} and the $MSE_{slope \cdot \Sigma}$ are higher for the Nexfin® signals, whereas the MSE_{Σ} is, as expected, higher for the IABP signals. Moderate correlations were found between the MSE_{Σ} of the MAP and DBP time series, the MSE_{slope} of the DBP time series, and the DBP $MSE_{slope \cdot \Sigma}$.

Table 6.6: Multiscale entropy measurements for the mean arterial blood pressure, diastolic blood pressure and systolic blood pressure registered with the invasive method and the Nexfin® device. It is presented the median, the first and third quartiles, the Spearman correlation (r_S) and the Wilcoxon test. P-values in bold are lower than 0.05.

	IABP	**Nexfin®**	**Spearman**		**Wilcoxon**
	Median (Q1, Q3)	**Median (Q1, Q3)**	**r (95% CI)**	**P**	**P**
MSE_{slope}, scale 1-5					
MAP	0.02 (-0.02, 0.01)	0.12 (0.07, 0.18)	0.50 (-0.05, 0.81)	0.072	**0.004**
DBP	0.04 (-0.01, 0.07)	0.09 (0.04, 0.13)	0.60 (0.11, 0.86)	**0.022**	**0.008**
SBP	0.03 (-0.05, 0.06)	0.08 (0.04, 0.13)	0.46 (-0.09, 0.80)	0.095	**0.019**
MSE_{Σ}, scale 1-5					
MAP	9.38 (8.64, 10.42)	8.44 (7.52, 8.88)	0.78 (0.43, 0.93)	**<0.001**	**0.003**
DBP	8.86 (7.94, 9.64)	8.30 (7.52, 8.71)	0.83 (0.54, 0.95)	**<0.001**	**0.036**
SBP	9.06 (8.66, 9.47)	8.53 (7.95, 9.14)	0.45 (-0.10, 0.79)	0.102	0.221
$MSE_{slope \cdot \Sigma}$					
MAP	0.26 (-0.24, 0.82)	0.92 (0.61, 1.46)	0.44 (-0.12, 0.79)	0.114	**0.009**
DBP	0.21 (-0.05, 0.53)	0.72 (0.31, 0.84)	0.63 (0.14, 0.87)	**0.017**	**0.013**
SBP	0.24 (-0.44, 0.55)	0.76 (0.30, 1.06)	0.44 (-0.12, 0.79)	0.118	**0.022**

Abbreviations: IABP, invasive arterial blood pressure; MAP, mean arterial blood pressure; DBP, diastolic blood pressure; SBP, systolic blood pressure; MSE, multiscale entropy.

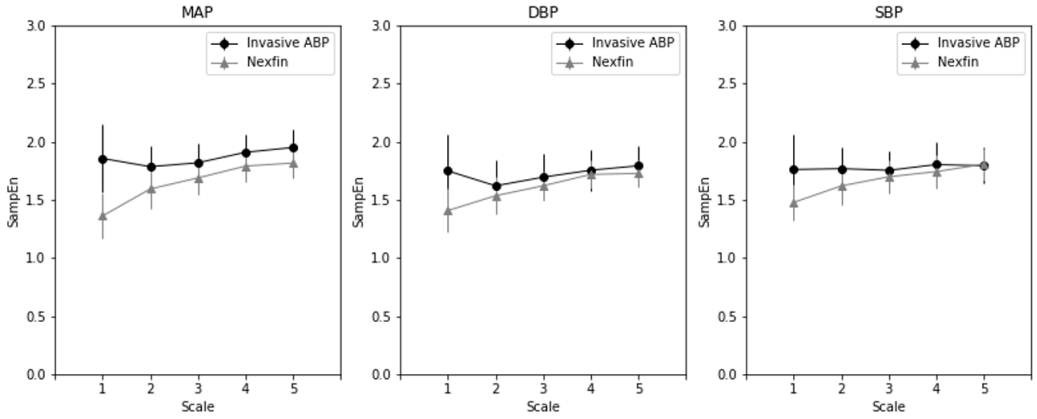

Figure 6.4: Sample entropy for scales 1 to 5 for the two methods: invasive arterial blood pressure (IABP) and Nexfin and for the three signal types: mean arterial blood pressure (MAP), diastolic blood pressure (DBP) and systolic blood pressure (SBP).

6.5 Compression analysis

Concerning the compression analysis done, it was computed the compression ratio for the scales 1 to 5. The values obtained for the two chosen compressors: GZIP and LZMA and the three different BP signals of the two methods are plotted in Figure 6.5. The ratio values between the two methods appear to be similar and, the higher the scale, the more concordant they tend to be.

The compression ration for the first scale and the three multiscale indices values for both IABP and Nexfin® time series are presented in Table 6.7.

For both compressors, the values registered for the scale 1 and the MSC_{Σ} between scales 1 and 5 are significantly higher for the signals acquired with the Nexfin® device. On the other hand, the MSC_{slope} and the $MSC_{slope \cdot \Sigma}$ values, are significantly higher for the IABP signals.

Overall, the high Spearman correlation values confirm the relation between the compression ration and the MSC_{slope} for the two methods. The scale 1 values for the two compressors have the highest values of correlation.

Figure 6.6 presents a comparison between the two compressors, where it is possible to see the range of their values and how the two BP measurement methods can be distinguished. The two compressors have very similar behavior for scale 1 of compression, and the slope between the 5 scales ratios have an almost linear correspondence. However, the $MSC_{slope \cdot \Sigma}$ has a quite disperse variation for the two methods.

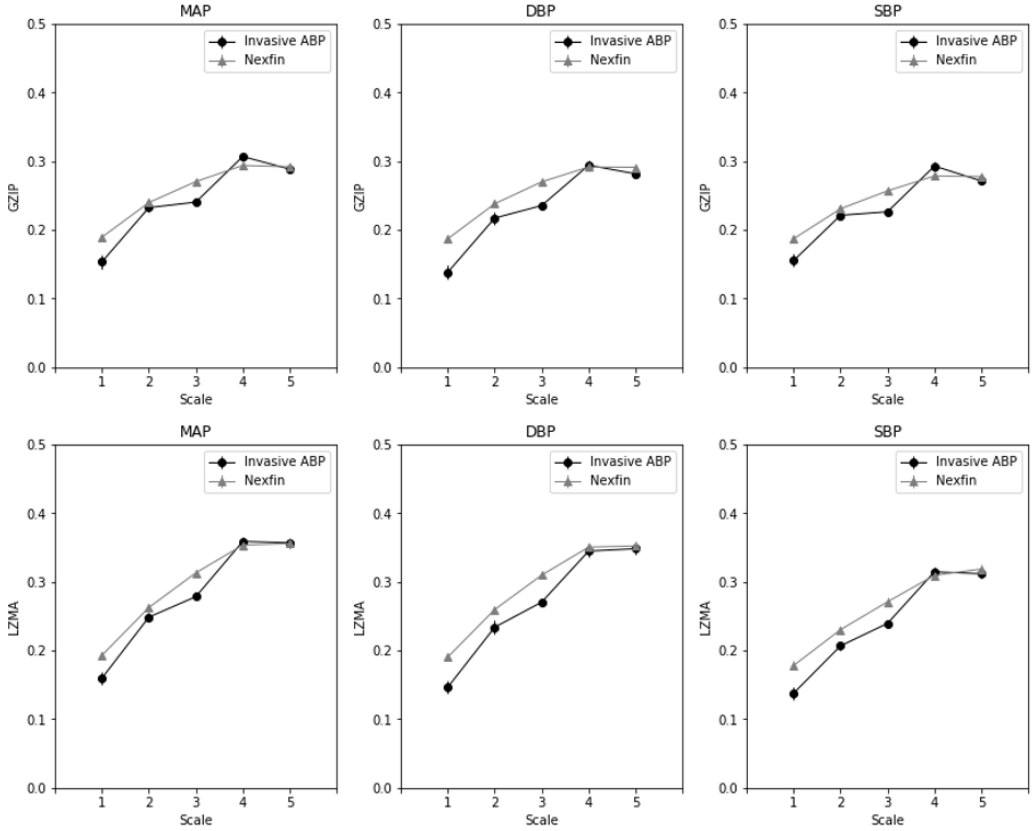

Figure 6.5: Compression ratio for scales 1 to 5 for the different signals (mean arterial blood pressure (MAP), diastolic blood pressure (DBP) and systolic blood pressure (SBP)) and for the GZIP and LZMA compressors.

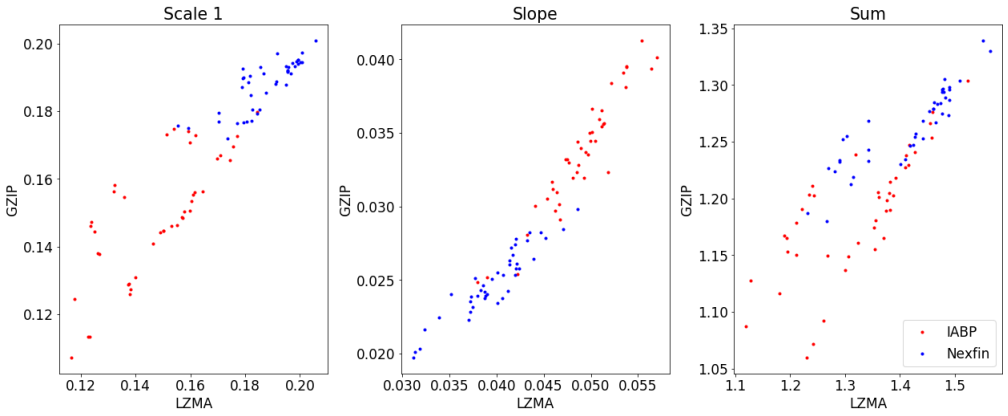

Figure 6.6: Comparison of the two chosen compressors when measuring the Scale 1 ratio, the MSC_{slope} and the MSC_{Σ} of the first five scales ratios.

Table 6.7: GZIP and LZMA compression measurements of IABP versus Noninvasive (Nexfin®) signals. P-values in bold are lower than 0.05

	IABP	**Nexfin®**	**Spearman**		**Wilcoxon**
	Median (Q1, Q3)	**Median (Q1, Q3)**	**r (95% CI)**	**P**	**P**
GZIP, scale 1					
MAP	0.155 (0.145, 0.167)	0.190 (0.186, 0.194)	0.87 (0.64, 0.96)	**<0.001**	**<0.001**
DBP	0.145 (0.126, 0.150)	0.193 (0.180, 0.194)	0.81 (0.48, 0.94)	**<0.001**	**<0.001**
SBP	0.156 (0.145, 0.172)	0.190 (0.181, 0.192)	0.82 (0.50, 0.94)	**<0.001**	**<0.001**
$GZIP_{slope}$, scale 1-5					
MAP	0.034 (0.032, 0.035)	0.026 (0.024, 0.027)	0.67 (0.22, 0.89)	**0.008**	**<0.001**
DBP	0.036 (0.034, 0.039)	0.026 (0.025, 0.027)	0.56 (0.04, 0.84)	**0.039**	**<0.001**
SBP	0.030 (0.028, 0.033)	0.024 (0.022, 0.024)	0.88 (0.65, 0.96)	**<0.001**	**<0.001**
$GZIP_{\Sigma}$, scale 1-5					
MAP	1.221 (1.193, 1.245)	1.284 (1.270, 1.296)	0.15 (-0.41, 0.63)	0.605	**0.002**
DBP	1.173 (1.150, 1.204)	1.282 (1.269, 1.296)	0.86 (0.61, 0.96)	**<0.001**	**<0.001**
SBP	1.166 (1.150, 1.200)	1.232 (1.220, 1.245)	0.40 (-0.16, 0.77)	0.154	**<0.001**
$GZIP_{slope \cdot \Sigma}$					
MAP	0.042 (0.040, 0.043)	0.034 (0.031, 0.035)	0.38 (-0.18, 0.76)	0.175	**<0.001**
DBP	0.043 (0.040, 0.044)	0.033 (0.033, 0.034)	0.30 (-0.27, 0.72)	0.296	**<0.001**
SBP	0.035 (0.033, 0.039)	0.029 (0.027, 0.030)	0.72 (0.30, 0.90)	**0.004**	**<0.001**
LZMA, scale 1					
MAP	0.161 (0.150, 0.171)	0.195 (0.188, 0.199)	0.93 (0.80, 0.98)	**<0.001**	**<0.001**
DBP	0.151 (0.138, 0.158)	0.195 (0.183, 0.198)	0.82 (0.51, 0.94)	**<0.001**	**<0.001**
SBP	0.132 (0.125, 0.153)	0.179 (0.173, 0.185)	0.82 (0.51, 0.94)	**<0.001**	**<0.001**
$LZMA_{slope}$, scale 1-5					
MAP	0.050 (0.049, 0.052)	0.042 (0.040, 0.042)	0.67 (0.22, 0.89)	**0.008**	**<0.001**
DBP	0.051 (0.050, 0.053)	0.041 (0.040, 0.043)	0.48 (-0.07, 0.81)	0.081	**<0.001**
SBP	0.046 (0.043, 0.048)	0.037 (0.033, 0.038)	0.84 (0.55, 0.95)	**<0.001**	**<0.001**
$LZMA_{\Sigma}$, scale 1-5					
MAP	1.399 (1.377, 1.417)	1.476 (1.447, 1.490)	0.29 (-0.28, 0.71)	0.311	**0.002**
DBP	1.358 (1.310, 1.380)	1.471 (1.456, 1.480)	0.62 (0.14, 0.87)	**0.018**	**<0.001**
SBP	1.211 (1.191, 1.239)	1.300 (1.284, 1.335)	-0.29 (-0.71, 0.28)	0.311	**0.001**
$LZMA_{slope \cdot \Sigma}$					
MAP	0.070 (0.067, 0.073)	0.060 (0.059, 0.064)	0.27 (-0.30, 0.70)	0.342	**0.003**
DBP	0.070 (0.066, 0.071)	0.060 (0.058, 0.062)	0.17 (-0.39, 0.64)	0.553	**0.002**
SBP	0.056 (0.051, 0.058)	0.048 (0.043, 0.051)	0.70 (0.27, 0.90)	**0.005**	**<0.001**

Abbreviations: IABP, invasive arterial blood pressure; MAP, mean arterial blood pressure; DBP, diastolic blood pressure; SBP, systolic blood pressure.

6.6 Association with the outputs: Linear regression

Linear regression models were done to relate the complexity and frequency parameters measured with the outputs. The values collected were the standardized linear regression coefficient, and its p value for all the IABP and Nexfin® signals.

Regarding the frequency measures, it was not found a statistically significant relationship between these parameters and the outputs. The results are present in Appendix D.

Table 6.8 compiles the linear regression information between the entropy measures (Shannon and sample entropies, MSE_{slope}, MSE_{Σ}, and $MSE_{slope\cdot\Sigma}$) and the STS morbidity and mortality risk. It was found a significant correlation for the MSE_{slope} and the $MSE_{slope\cdot\Sigma}$, for the DBP of the invasive method and all the Nexfin®'s signals.

Regarding the compression measures association with the outputs, it was only found statistically relevant results for the association with the ICU length of time. Table 6.9 shows the results collected. It is possible to see that the MSC_{scale1} and MSC_{Σ} where the parameters with the most significant results and that the two compressors used showed a very similar behavior.

Table 6.8: Linear regression standardized coefficients and 95% CI for the association between the entropy values (SampEn, Shannon entropy, and MSE) and the logaritmically transformed STS risk for each blood pressure signal. P-values in bold are lower than 0.05.

	log10 STS risk			
	Coefficient (95% CI)			
	IABP		**Nexfin®**	
Shannon				
MAP	0.51 (-1.62, 2.64)	0.603	2.00 (-0.49, 4.49)	0.104
DBP	0.66 (-1.44, 2.76)	0.498	1.82 (-0.53, 4.16)	0.115
SBP	0.39 (-1.91, 2.68)	0.715	1.32 (-1.24, 3.88)	0.276
SampEn				
MAP	2.13 (0.20, 4.06)	**0.034**	2.48 (-0.24, 5.21)	0.070
DBP	0.90 (-0.68, 2.48)	0.233	1.93 (-0.89, 4.75)	0.159
SBP	1.14 (-0.34, 2.62)	0.118	2.47 (-1.27, 6.22)	0.172
MSE_{slope}				
MAP	-5.73 (-11.95, 0.49)	0.067	-12.55 (-19.65, -5.45)	**0.003**
DBP	-8.68 (-15.30, -2.06)	**0.015**	-10.29 (-19.59, -1.00)	**0.033**
SBP	-1.53 (-9.28, 6.22)	0.670	-9.28 (-18.06, -0.49)	**0.041**
MSE_{Σ}				
MAP	0.42 (-0.07, 0.90)	0.084	0.19 (-0.35, 0.73)	0.454
DBP	0.18 (-0.21, 0.58)	0.327	0.22 (-0.35, 0.80)	0.404
SBP	0.39 (-0.08, 0.86)	0.094	0.22 (-0.36, 0.80)	0.418
$MSE_{slope\cdot\Sigma}$				
MAP	-0.60 (-1.23, 0.03)	0.059	-1.32 (-2.20, -0.44)	**0.008**
DBP	-0.86 (-1.53, -0.20)	**0.016**	-1.37 (-2.50, -0.24)	**0.022**
SBP	-0.14 (-1.01, 0.74)	0.731	-1.07 (-2.11, -0.02)	**0.046**

Abbreviations: IABP, invasive arterial blood pressure; MAP, mean arterial blood pressure; DBP, diastolic blood pressure; SBP, systolic blood pressure; MSE, multiscale entropy; CI, confidence interval; STS, society of thoracic surgeons; SampEn, sample entropy.

Table 6.9: Linear regression standardized coefficients and 95% CI for the association between the compression measures and the logaritmically transformed ICU time for each blood pressure signal. P-values in bold are lower than 0.05.

	log10 ICU time			
	Coefficient (95% CI)			
	IABP		**Nexfin®**	
$GZIP_{scale1}$				
MAP	53.45 (14.17, 92.74)	**0.012**	113.01 (19.94, 206.09)	**0.022**
DBP	54.12 (17.95, 90.30)	**0.007**	88.33 (14.57, 162.08)	**0.023**
SBP	38.97 (-0.76, 78.70)	0.054	63.17 (-27.50, 153.84)	0.153
$GZIP_{slope}$				
MAP	-187.23 (-398.78, 24.32)	0.077	-195.81 (-488.89, 97.27)	0.169
DBP	-354.58 (-577.65, -131.51)	**0.005**	-533.06 (-940.24, -125.88)	**0.015**
SBP	-62.80 (-244.23, 118.63)	0.462	-129.72 (-480.64, 221.19)	0.433
$GZIP_{\Sigma}$				
MAP	16.56 (1.85, 31.27)	**0.031**	13.75 (-10.58, 38.09)	0.239
DBP	12.63 (1.69, 23.56)	**0.027**	26.97 (0.19, 53.75)	**0.049**
SBP	15.62 (-0.16, 31.40)	**0.052**	13.61 (-12.32, 39.55)	0.272
$GZIP_{slope \cdot \Sigma}$				
MAP	-102.29 (-298.89, 94.31)	0.276	-84.80 (-287.82, 118.22)	0.378
DBP	-187.11 (-430.82, 56.61)	0.119	-339.42 (-692.36, 13.52)	0.058
SBP	-19.65 (-185.24, 145.95)	0.799	-73.51 (-339.46, 192.44)	0.555
$LZMA_{scale1}$				
MAP	58.37 (15.20, 101.53)	**0.013**	88.83 (9.78, 167.89)	**0.031**
DBP	54.05 (15.96, 92.15)	**0.010**	92.16 (22.25, 162.08)	**0.014**
SBP	40.12 (-0.20, 80.44)	0.051	67.94 (10.92, 124.97)	**0.024**
$LZMA_{slope}$				
MAP	-76.15 (-292.00, 139.71)	0.454	-78.26 (-291.22, 134.70)	0.436
DBP	-309.96 (-544.44, -75.48)	**0.014**	-218.14 (-477.90, 41.61)	0.092
SBP	-54.40 (-222.92, 114.11)	0.492	-55.3 (-245.15, 134.55)	0.535
$LZMA_{\Sigma}$				
MAP	14.85 (2.92, 26.78)	**0.019**	7.79 (-8.02, 23.60)	0.301
DBP	10.74 (0.98, 20.49)	**0.034**	16.76 (-4.09, 37.61)	0.105
SBP	11.36 (-0.94, 23.66)	0.067	16.15 (1.95, 30.36)	0.029
$LZMA_{slope \cdot \Sigma}$				
MAP	16.23 (-103.07, 135.52)	0.770	-17.83 (-127.76, 92.11)	0.728
DBP	-37.83 (-185.59, 109.93)	0.584	-87.34 (-257.54, 82.86)	0.283
SBP	13.57 (-116.95, 144.09)	0.823	5.27 (-115.43, 125.97)	0.925

Abbreviations: IABP, invasive arterial blood pressure; MAP, mean arterial blood pressure; DBP, diastolic blood pressure; SBP, systolic blood pressure; CI, confidence interval; ICU, intensive care unit.

Chapter 7

Discussion

This chapter presents the discussion and interpretation of the results obtained and described in Chapter 6. The results are also compared to previous studies in the same area, and some suggestions are laid out to improve future work.

In general, the results obtained show that the BP values obtained with the measurement methods are similar and related. In addition, they proved that the signals collected with the Nexfin device could be linked to the outcomes: the STS morbidity and mortality score, the EUROScore, and the time spent in the ICU.

The mean and standard deviation values are similar for the invasive and non-invasive signals. However, it can be observed that the higher the BP, the lower is the mean difference, and the higher is the standard deviation and its difference. Visually, it is possible to note that the invasive signals appear to be more constant with a well-defined variance range. Moreover, the standard deviation is, in general, higher with the Nexfin device. This variation might be explained by the presence of unwanted artifacts in the Nexfin signals or can be a consequence of a higher sensibility of the device that may imply the existence of more information that can be relevant. Also, it may be concluded that the non-invasive method may have reduced accuracy in lower pressures.

However, the Wilcoxon paired test showed that mean values between the two methods are related for the MAP and the DBP signals. Combining these two pieces of information, it can be concluded that the MAP and DBP signals have a relatively constant vertical shift between the two measurements. The same does not happen for the SBP.

Opposingly, when, in 2009, Eeftinck et al. compared the Nexfin device with the auscultatory method, it was noted a higher mean difference for the SBP signals [55]. Furthermore, the difference values between the two methods that they recorded were considerably lower than the ones registered in this study. In 2010, Martina et al. also registered a lower difference between the mean BP value acquired with the Nexfin device and the invasive radial BP.

When comparing the signals obtained with the CNAP device with the IABP, in the study by Gibson et al. in 2018 [4], the average values observed for the DBP and MAP were also higher for the CNAP signals and the SBP signals' mean was similar, likewise. The mean difference values

are very identical to what was observed in this study but the standard deviation differences are considerably lower.

Regarding the frequency analysis, the observation of the areas of the HF and MF ranges of the spectrum, made it possible to conclude that they are related and that the Nexfin device conserves information on the frequency of the signals. The DBP signal were the ones who registered the bigger difference between the two methods that can be interpreted by its higher susceptibility to the presence of noise and by its lower signal to noise ratio. None of the collected values showed significant association with the outputs.

The coherence analysis demonstrated, once again, that the two methods are related frequency-wise and showed that this value is higher for the MF range for the 3 signals. Being the MF range the one associated with the Mayer waves, a higher coherence of the two signals means that there is conservation of the information on the risk of cardiovascular diseases.

For the entropy analysis of the signals, the parameter that had the most promising results was the Shannon entropy where the two measuring methods present very similar and correlated results. In addition, it is possible to conclude that, the greater the BP, the greater is the Shannon entropy.

Regarding the sample entropy and the MSE, the results are similar to those obtained by Gibson et al. in 2018[4] for the CNAP device. The Nexfin and the CNAP devices registered a lower value for the MSE_{Σ} and a higher value for the MSE_{slope}, when compared to the IABP signal. As mentioned in their study, this might imply that there is a certain attenuation of the variability of the signal, possible due to filtering. The correlation of these parameters with the outputs was also very notable, especially for the MSE_{slope} and the $MSE_{slope\cdot\Sigma}$ of the non-invasive signals. The parameters were negatively associated with the output, as expected, since the signals complexity decreases with the increase of the risk associated, usually related with aging and disease [4].

It could be expected that the Nexfin device would not capture the characteristic complexity of the signal like the invasive method. However, while the sample entropy is slightly higher for the IABP, the Shannon entropy is higher for the non-invasive method. It is possible to conclude that the dynamical complexity of the signals is overall preserved.

As respects the compression analysis, the compression ratio is, generally, higher for the Nexfin device meaning that its signals contain more unstructured information than the IABP signals. Comparing the two compressors used, the LZMA compressor is able to correlate both methods more efficiently for the first scale. However, if more scales are studied and the slope and sum parameters are used, then the two compressors are very similar and the GZIP compressor might have slightly better results.

In general, compression measures showed to describe relevant information that is preserved in the non-invasive signals and that is also correlated with time spent by the patient in the ICU. Of all the collected compression parameters, the scale 1 of the compression revealed the most statistically significant association with the mentioned output.

All in all, the entropy measures are better correlated with the STS morbidity and mortality risk, whereas, the compression measures have a stronger association with the patient's time in the ICU.

This way, the complexity preserved in the signals can be measured and used to infer the patient's health.

Throughout this work, several limitations were noted, especially regarding the population used for this study. It is important to refer that there were used only 14 patients who provide a very limited variability of signals acquired. Of those 14 patients, only one was female, being the gender distribution very unequal. Furthermore, and since the STS mortality and morbidity risk score is only computed for patients indicated for CAB, aortic or mitral valve procedures, the sample size was reduced to 12 patients for every calculation that included these risk value.

The signals collected also have different lengths and duration, meaning that certain information was lost, mainly on the invasive signals, when the signals were synchronized. Moreover, the synchronization process was not efficient since it required a manual adjustment.

In addition, some studies refer to the necessity of large sample sizes to have accurate calculations of the correlation coefficients. For instance, the Pearson correlation coefficient can be used for sample sizes larger than 6 but should only be used for sizes above 25 [82, 83]. Therefore, in this study, some parameters might be over or under-estimated.

In future works, some aspects should be improved, and some other areas could be examined. It should be used a larger and more diverse population that allowed for results with more statistical significance.

Furthermore, it is important to have a mechanism that collects both signals simultaneously or that provides an automatic synchronization process based on the matching of patterns between signals, so that a manual synchronization process is not required.

The pre-processing of Nexfin signals could be more explored by doing some filtering or by removing the baseline. The Nexfin provides unreconstructed signals that, as mentioned before, do not go through a processing operation (non disclosed), unlike the signals used. It could be interesting to test the same measures for these signals and see if the processing operation removed crucial information present in the IABP signals.

Furthermore, once the Nexfin provides the heart rate information, it could be of interest to test out how this can be associated with the BP signals and the outputs. The same could be done for several other values like the cardiac index, the systemic vascular resistance, the cardiac output or the stroke volume.

In conclusion, this work can be broadened to several more parameters to find to what extent the Nexfin device preserves the information given by the traditional methods.

Chapter 8

Conclusion

Blood pressure is a vital biological signal with high importance once it can be an indicator of several cardiovascular problems and risks. The goal of this work was to validate the Nexfin device of the *ClearSight System* that is able to collect BP signals continuously, in a preoperative setting, without being an invasive method. Unlike previous studies, this work used linear and non-linear methodologies to evaluate the dynamic of the temporal series and compare the acquired parameters with 3 different outputs related to surgery and cardiovascular risk.

It was used time-domain measures, frequency measures, complexity measures that included a entropy and compression analysis, and it was performed a linear regression to establish an association of these parameters with the STS morbidity, and mortality risk score, the EUROScore and the time spent in the ICU by the patient.

For all the parameters collected, there were differences found between the invasive and the non-invasive method. However, many were highly correlated. Furthermore, a correlation was found between entropy parameters and the STS morbidity and mortality risk score, and also between the compression measures and the time spent in the ICU. Therefore, the study concludes that the Nexfin device preserves information in its time, frequency, and complexity dimensions that can be analyzed since it is coherent with the information of the invasive signals.

Accordingly, and being the utmost goal to introduce this device in the medical routines, this work revealed that the Nexfin device captures the dynamic of the signals collected and also the information necessary to safeguard the patient's health.

Several other parameters could be analyzed in future work, including the patient's heart rate or cardiac output.

References

[1] Prospective Studies Collaboration et al. Age-specific relevance of usual blood pressure to vascular mortality: a meta-analysis of individual data for one million adults in 61 prospective studies. *Lancet*, 360(9349):1903–1913, 2002.

[2] Jeremy Booth. *A short history of blood pressure measurement*. SAGE Publications, 1977.

[3] Agnes S Meidert and Bernd Saugel. Techniques for non-invasive monitoring of arterial blood pressure. *Frontiers in medicine*, 4:231, 2018.

[4] Henriques T. S. Costa M. D. Davis R. B. Mittleman M. A. Mathur P. Subramaniam B. Gibson, L. E. Comparison of invasive and noninvasive blood pressure measurements for assessing signal complexity and surgical risk in cardiac surgical patients. *Anesthesia Analgesia*, 1, 2018.

[5] Settels J. Perel A., Wesselink W. The nexfin monitor — a totally non-invasive cardiac output monitor. *Gullo A. (eds) Anaesthesia, Pharmacology, Intensive Care and Emergency Medicine A.P.I.C.E.. Springer, Milano*, 2011.

[6] Jerson R Martina, Berend E Westerhof, Jeroen van Goudoever, Edouard MF H de Beaumont, Jasper Truijen, Yu-Sok Kim, Rogier V Immink, Dorothea A Jöbsis, Markus W Hollmann, Jaap R Lahpor, et al. Noninvasive continuous arterial blood pressure monitoring with nexfin®. *Anesthesiology: The Journal of the American Society of Anesthesiologists*, 116(5):1092–1103, 2012.

[7] Jerson R Martina, Berend E Westerhof, Jeroen Van Goudoever, Nicolaas De Jonge, Johannes J Van Lieshout, Jaap R Lahpor, and Bas AJM De Mol. Noninvasive blood pressure measurement by the nexfin monitor during reduced arterial pulsatility: a feasibility study. *ASAIO journal*, 56(3):221–227, 2010.

[8] Alain F Kalmar, Jaap Jan Vos, Marloes Weening, Eline A Mooyaart, Marieke Poterman, MMRF Struys, and Thomas WL Scheeren. Validation of continuous noninvasive arterial blood pressure measurements during general anesthesia. *A174*, 14, 2012.

[9] MO Fischer, R Avram, I Cârjaliu, Massimo Massetti, JL Gérard, JL Hanouz, and JL Fellahi. Non-invasive continuous arterial pressure and cardiac index monitoring with nexfin after cardiac surgery. *British journal of anaesthesia*, 109(4):514–521, 2012.

[10] Serban Ion Bubenek-Turconi, Mihaela Craciun, Ion Miclea, and Azriel Perel. Noninvasive continuous cardiac output by the nexfin before and after preload-modifying maneuvers: a comparison with intermittent thermodilution cardiac output. *Anesthesia & Analgesia*, 117(2):366–372, 2013.

[11] O Broch, J Renner, M Gruenewald, P Meybohm, J Schöttler, A Caliebe, M Steinfath, M Malbrain, and B Bein. A comparison of the nexfin® and transcardiopulmonary thermodilution to estimate cardiac output during coronary artery surgery. *Anaesthesia*, 67(4):377–383, 2012.

[12] Roberto M Lang, Michelle Bierig, Richard B Devereux, Frank A Flachskampf, Elyse Foster, Patricia A Pellikka, Michael H Picard, Mary J Roman, James Seward, Jack Shanewise, et al. Recommendations for chamber quantification. *European journal of echocardiography*, 7(2):79–108, 2006.

[13] Randall S Stafford. New high blood pressure guidelines: back on track with lower treatment goals, but implementation challenges abound, 2018.

[14] Jeremiah Stamler, Rose Stamler, and James D Neaton. Blood pressure, systolic and diastolic, and cardiovascular risks: Us population data. *Archives of internal medicine*, 153(5):598–615, 1993.

[15] Alexander A Leung, Stella S Daskalopoulou, Kaberi Dasgupta, Kerry McBrien, Sonia Butalia, Kelly B Zarnke, Kara Nerenberg, Kevin C Harris, Meranda Nakhla, Lyne Cloutier, et al. Hypertension canada's 2017 guidelines for diagnosis, risk assessment, prevention, and treatment of hypertension in adults. *Canadian Journal of Cardiology*, 33(5):557–576, 2017.

[16] Mafalda Santos and Teresa Rodrigues. A hipertensão arterial na urgência. *Revista Portuguesa de Medicina Geral e Familiar*, 24(3):411–7, 2008.

[17] Jeremiah Stamler, James D Neaton, and Deborah N Wentworth. Blood pressure (systolic and diastolic) and risk of fatal coronary heart disease. *Hypertension*, 13(5_supplement):I2, 1989.

[18] L Abraham-Inpijn, A Borgmeijer-Hoelen, and RA Th Gortzak. Changes in blood pressure, heart rate, and electrocardiogram during dental treatment with use of local anesthesia. *The Journal of the American Dental Association*, 116(4):531–536, 1988.

[19] John S Floras. Blood pressure variability: a novel and important risk factor. *Canadian Journal of Cardiology*, 29(5):557–563, 2013.

[20] Ding-Feng Su and Chao-Yu Miao. Reduction of blood pressure variability: a new strategy for the treatment of hypertension. *Trends in pharmacological sciences*, 26(8):388–390, 2005.

[21] Christian Höcht. Blood pressure variability: prognostic value and therapeutic implications. *ISRN Hypertension*, 2013, 2013.

[22] JS Floras, MO Hassan, PS Sever, JV Jones, B Osikowska, and P Sleight. Cuff and ambulatory blood pressure in subjects with essential hypertension. *The Lancet*, 318(8238):107–109, 1981.

[23] John S Floras, M Osman Hassan, J Vann Jones, Barbara A Osikowska, Peter S Sever, and Peter Sleight. Factors influencing blood pressure and heart rate variability in hypertensive humans. *Hypertension*, 11(3):273–281, 1988.

[24] Gianfranco Parati, Juan E Ochoa, Carolina Lombardi, and Grzegorz Bilo. Assessment and management of blood-pressure variability. *Nature Reviews Cardiology*, 10(3):143, 2013.

[25] Andrew JS Coats, James Conway, Peter Sleight, Theo E Meyer, Virend K Somers, John S Floras, and John Vann Jones. Interdependence of blood pressure and heart period regulation in mild hypertension. *American journal of hypertension*, 4(3_Pt_1):234–238, 1991.

[26] Saeid R Seydnejad and Richard I Kitney. Modeling of mayer waves generation mechanisms. *IEEE Engineering in Medicine and Biology Magazine*, 20(2):92–100, 2001.

[27] Reijo Takalo, Ilkka Korhonen, Silja Majahalme, Martti Tuomisto, and Väinö Turjanmaa. Circadian profile of low-frequency oscillations in blood pressure and heart rate in hypertension. *American journal of hypertension*, 12(9):874–881, 1999.

[28] Gianfranco Parati, Guido Pomidossi, Fabio Albini, Daniele Malaspina, and Giuseppe Mancia. Relationship of 24-hour blood pressure mean and variability to severity of target-organ damage in hypertension. *Journal of hypertension*, 5(1):93–98, 1987.

[29] Martin E Young. The circadian clock within the heart: potential influence on myocardial gene expression, metabolism, and function. *American Journal of Physiology-Heart and Circulatory Physiology*, 290(1):H1–H16, 2006.

[30] Paul E Drawz, Mohamed Abdalla, and Mahboob Rahman. Blood pressure measurement: clinic, home, ambulatory, and beyond. *American Journal of Kidney Diseases*, 60(3):449–462, 2012.

[31] LA Geddes and LE Baker. Principles of applied biomedical instrumentation. *American Journal of Physical Medicine & Rehabilitation*, 49(5):317, 1970.

[32] Chung-Hsien Kuo, Chun-Ju Wu, Hung-Chyun Chou, Guan-Ting Chen, and Yu-Cheng Kuo. Development of a blood pressure measurement instrument with active cuff pressure control schemes. *Journal of healthcare engineering*, 2017, 2017.

[33] Kurt Barbé, Wendy Van Moer, and Lieve Lauwers. Oscillometric blood pressure measurements: A signal analysis. In *Journal of Physics: Conference Series*, volume 238, page 012052. IOP Publishing, 2010.

[34] A Ball-Llovera, R Del Rey, R Ruso, J Ramos, O Batista, and I Niubo. An experience in implementing the oscillometric algorithm for the noninvasive determination of human blood pressure. In *Proceedings of the 25th Annual International Conference of the IEEE Engineering in Medicine and Biology Society (IEEE Cat. No. 03CH37439)*, volume 4, pages 3173–3175. IEEE, 2003.

[35] Josep Sola, Mattia Bertschi, and Jens Krauss. Measuring pressure: Introducing obpm, the optical revolution for blood pressure monitoring. *IEEE pulse*, 9(5):31–33, 2018.

[36] GL Pressman and PM Newgard. A transducer for the continuous external measurement of arterial blood pressure. *IEEE Transactions on Bio-Medical Electronics*, 10(2):73–81, 1963.

[37] VE Antsiperov and GK Mansurov. Continuous non-invasive arterial blood pressure monitor with active sensor architecture. *Int. J. Adv. Life Sci*, 8(3-4):289–296, 2016.

[38] J Penaz, A Voigt, and W Teichmann. Contribution to the continuous indirect blood pressure measurement. *Zeitschrift fur die gesamte innere Medizin und ihre Grenzgebiete*, 31(24):1030–1033, 1976.

[39] RJO Davies, NE Jenkins, and JR Stradling. Effect of measuring ambulatory blood pressure on sleep and on blood pressure during sleep. *Bmj*, 308(6932):820–823, 1994.

[40] C Ilies, H Kiskalt, D Siedenhans, P Meybohm, M Steinfath, B Bein, and R Hanss. Detection of hypotension during caesarean section with continuous non-invasive arterial pressure device or intermittent oscillometric arterial pressure measurement. *British journal of anaesthesia*, 109(3):413–419, 2012.

[41] Alena Stenglova and Jan Benes. Continuous non-invasive arterial pressure assessment during surgery to improve outcome. *Frontiers in medicine*, 4:202, 2017.

[42] Markus V Küntscher, Sigrid Blome-Eberwein, Michael Pelzer, Detlev Erdmann, and Günter Germann. Transcardiopulmonary vs pulmonary arterial thermodilution methods for hemodynamic monitoring of burned patients. *The Journal of burn care & rehabilitation*, 23(1):21–26, 2002.

[43] Kanu Chatterjee. The swan-ganz catheters: past, present, and future: a viewpoint. *Circulation*, 119(1):147–152, 2009.

[44] Thomas J Kearney and M Michael Shabot. Pulmonary artery rupture associated with the swan-ganz catheter. *Chest*, 108(5):1349–1352, 1995.

[45] Christer Svensen and Peter Rodhe. Intravascular volume replacement therapy. In *Pharmacology and Physiology for Anesthesia*, pages 795–813. Elsevier, 2019.

[46] Nicolo Piazza, Peter Wenaweser, Menno van Gameren, Thomas Pilgrim, Apostolos Tsikas, Amber Otten, Rutger Nuis, Yoshinobu Onuma, Jin Ming Cheng, A Pieter Kappetein, et al. Relationship between the logistic euroscore and the society of thoracic surgeons predicted risk of mortality score in patients implanted with the corevalve revalving system—a bern-rotterdam study. *American heart journal*, 159(2):323–329, 2010.

[47] MAJID Maleki. *Evaluation of patients with cardiovascular problems*. Elsevier Health Sciences, 2017.

[48] H Karabulut, F Toraman, C Alhan, G Camur, S Evrenkaya, S Dağdelen, and S Tarcan. Euroscore overestimates the cardiac operative risk. *Cardiovascular Surgery*, 11(4):295–298, 2003.

[49] Ben PM Imholz, Wouter Wieling, Gert A van Montfrans, and Karel H Wesseling. Fifteen years experience with finger arterial pressure monitoring: assessment of the technology. *Cardiovascular research*, 38(3):605–616, 1998.

[50] Ben PM Imholz, Jos J Settels, Anton H van der Meiracker, Karel H Wesseling, and Wouter Wieling. Non-invasive continuous finger blood pressure measurement during orthostatic stress compared to intra-arterial pressure. *Cardiovascular research*, 24(3):214–221, 1990.

[51] Willem Jan W Bos, Ben PM Imholz, Jeroen van Goudoever, Karel H Wesseling, and Gert A van Montfrans. The reliability of noninvasive continuous finger blood pressure measurement in patients with both hypertension and vascular disease. *American journal of hypertension*, 5(8):529–535, 1992.

[52] J Penaz. Photoelectric measurement of blood pressure, volume and flow in the finger'in: Digest of the 10th international conference on medical and biological engineering. *Dresden*, 104, 1973.

[53] KH Wesseling. Physiocal, calibrating finger vascular physiology for finapres. *Homeostasis*, 36:67–82, 1995.

[54] Paolo Gizdulich, Andriana Prentza, and Karel H Wesseling. Models of brachial to finger pulse wave distortion and pressure decrement. *Cardiovascular research*, 33(3):698–705, 1997.

[55] Daan W Eeftinck Schattenkerk, Johannes J Van Lieshout, Anton H Van Den Meiracker, Karel R Wesseling, Stéphane Blanc, Wouter Wieling, Gert A Van Montfrans, Jos J Settels, Karel H Wesseling, and Berend E Westerhof. Nexfin noninvasive continuous blood pressure validated against riva-rocci/korotkoff. *American journal of hypertension*, 22(4):378–383, 2009.

[56] Richard M Nowak, Ayan Sen, Audwin J Garcia, Heidi Wilkie, James J Yang, Michael R Nowak, and Michele L Moyer. The inability of emergency physicians to adequately clinically estimate the underlying hemodynamic profiles of acutely ill patients. *The American journal of emergency medicine*, 30(6):954–960, 2012.

[57] J Akkermans, M Diepeveen, W Ganzevoort, GA Van Montfrans, BE Westerhof, and H Wolf. Continuous non-invasive blood pressure monitoring, a validation study of nexfin in a pregnant population. *Hypertension in pregnancy*, 28(2):230–242, 2009.

[58] A Voss, V Baier, S Schulz, and KJ Bar. Linear and nonlinear methods for analyses of cardiovascular variability in bipolar disorders. *Bipolar disorders*, 8(5p1):441–452, 2006.

[59] Solange Akselrod, David Gordon, F Andrew Ubel, Daniel C Shannon, AC Berger, and Richard J Cohen. Power spectrum analysis of heart rate fluctuation: a quantitative probe of beat-to-beat cardiovascular control. *science*, 213(4504):220–222, 1981.

[60] Pascale Mansier, Jean Clairambault, Nathalie Charlotte, Claire Médigue, Christophe Vermeiren, Gilles LePape, François Carré, Athanassia Gounaropoulou, and Bernard Swynghedauw. Linear and non-linear analyses of heart rate variability: a minireview. *Cardiovascular Research*, 31(3):371–379, 1996.

[61] Zsolt Őri, George Monir, Jerry Weiss, Xavier Sayhouni, and Donald H Singer. Heart rate variability: frequency domain analysis. *Cardiology clinics*, 10(3):499–533, 1992.

[62] KAZUHIRO Inoue, SHINJI Miyake, MASAHARU Kumashiro, HAJIME Ogata, TAKAYOSHI Ueta, and TAKASHI Akatsu. Power spectral analysis of blood pressure variability in traumatic quadriplegic humans. *American Journal of Physiology-Heart and Circulatory Physiology*, 260(3):H842–H847, 1991.

[63] Gianfranco Parati, J Philip Saul, Marco Di Rienzo, and Giuseppe Mancia. Spectral analysis of blood pressure and heart rate variability in evaluating cardiovascular regulation: a critical appraisal. *Hypertension*, 25(6):1276–1286, 1995.

[64] Karim Ansari-Asl, Lotfi Senhadji, Jean-Jacques Bellanger, and Fabrice Wendling. Quantitative evaluation of linear and nonlinear methods characterizing interdependencies between brain signals. *Physical Review E*, 74(3):031916, 2006.

[65] Timo H Mäkikallio, Jari M Tapanainen, Mikko P Tulppo, and Heikki V Huikuri. Clinical applicability of heart rate variability analysis by methods based on nonlinear dynamics. *Cardiac electrophysiology review*, 6(3):250–255, 2002.

[66] Teresa Henriques, Hernâni Gonçalves, Luís Antunes, Mara Matias, João Bernardes, and Cristina Costa-Santos. Entropy and compression: two measures of complexity. *Journal of Evaluation in Clinical Practice*, 19(6):1101–1106, 2013.

[67] Claude E Shannon. A mathematical theory of communication. *Bell system technical journal*, 27(3):379–423, 1948.

[68] Yongbo Li, Xianzhi Wang, Zhenbao Liu, Xihui Liang, and Shubin Si. The entropy algorithm and its variants in the fault diagnosis of rotating machinery: A review. *IEEE Access*, 6:66723–66741, 2018.

[69] Steven M Pincus. Approximate entropy as a measure of system complexity. *Proceedings of the National Academy of Sciences*, 88(6):2297–2301, 1991.

[70] Joshua S Richman and J Randall Moorman. Physiological time-series analysis using approximate entropy and sample entropy. *American Journal of Physiology-Heart and Circulatory Physiology*, 278(6):H2039–H2049, 2000.

[71] Madalena Costa, Ary L Goldberger, and C-K Peng. Multiscale entropy analysis of complex physiologic time series. *Physical review letters*, 89(6):068102, 2002.

[72] Michael A Busa and Richard EA van Emmerik. Multiscale entropy: A tool for understanding the complexity of postural control. *Journal of Sport and Health Science*, 5(1):44–51, 2016.

[73] Andrei Nikolaevich Kolmogorov. Three approaches to the definition of the concept "quantity of information". *Problemy peredachi informatsii*, 1(1):1–11, 1965.

[74] Jacob Ziv and Abraham Lempel. A universal algorithm for sequential data compression. *IEEE Transactions on information theory*, 23(3):337–343, 1977.

[75] David A Huffman. A method for the construction of minimum-redundancy codes. *Proceedings of the IRE*, 40(9):1098–1101, 1952.

[76] J Martin Bland and DouglasG Altman. Statistical methods for assessing agreement between two methods of clinical measurement. *The lancet*, 327(8476):307–310, 1986.

[77] A Martin Andrés, I Herranz Tejedor, and A Silva Mato. The wilcoxon, spearman, fisher, χ2-, student and pearson tests and 2 times 2 tables. *Journal of the Royal Statistical Society: Series D (The Statistician)*, 44(4):441–450, 1995.

[78] Mavuto M Mukaka. A guide to appropriate use of correlation coefficient in medical research. *Malawi medical journal*, 24(3):69–71, 2012.

[79] Charles Spearman. The proof and measurement of association between two things. 1961.

[80] Frank Wilcoxon. Individual comparisons by ranking methods. In *Breakthroughs in statistics*, pages 196–202. Springer, 1992.

[81] Teresa S Henriques, Madalena D Costa, Pooja Mathur, Priyam Mathur, Roger B Davis, Murray A Mittleman, Kamal R Khabbaz, Ary L Goldberger, and Balachundhar Subramaniam. Complexity of preoperative blood pressure dynamics: possible utility in cardiac surgical risk assessment. *Journal of clinical monitoring and computing*, 33(1):31–38, 2019.

[82] Douglas G Bonett and Thomas A Wright. Sample size requirements for estimating pearson, kendall and spearman correlations. *Psychometrika*, 65(1):23–28, 2000.

[83] Florence Nightingale David. *Tables of the ordinates and probability integral of the distribution of the correlation coefficient in small samples*. Cambridge University Press, 1938.

[84] Eoin O'Brien, Thomas Pickering, Roland Asmar, Martin Myers, Gianfranco Parati, Jan Staessen, Thomas Mengden, Yutaka Imai, Bernard Waeber, Paolo Palatini, et al. Working group on blood pressure monitoring of the european society of hypertension international protocol for validation of blood pressure measuring devices in adults. *Blood pressure monitoring*, 7(1):3–17, 2002.

Appendix A

European Society of Hypertension validation procedure phases

Table A.1: Requirements to pass Phase 1 of the European Society of Hypertension validation procedure [84]. At least one of the following 3 conditions must be verified.

	Number of measurements	Values within	Condition
Phase 1	25/45	5 mmHg	1
	35/45	10 mmHg	2
	40/45	15 mmHg	3

Table A.2: Requirements to pass Phase 2.1 of the European Society of Hypertension validation procedure [84]. The conditions 1, 2 and 3 must be simultaneously verified and 2 out of the conditions 4, 5 and 6 must be confirmed.

	Number of comparisons	Values within	Condition
Phase 2.1	60/99	5 mmHg	1
	75/99	10 mmHg	2
	90/99	15 mmHg	3
	65/99	5 mmHg	4
	80/99	10 mmHg	5
	95/99	15 mmHg	6

Table A.3: Requirements to pass Phase 2.2 of the European Society of Hypertension validation procedure [84]. The conditions must both be simultaneously verified.

	Number of patients	Number of measurements	Values	Condition
Phase 2.2	$\geq 22/33$	2/3	within 5 mmHg	1
	<3/33	3/3	>5 mmHg	2

Appendix B

Demographic and clinic characterization of the subjects

Table B.1: Demographic and clinic characterization of the subjects to be used on the dissertation project.

Patient	Gender	Age	Procedure	STS mortality/ morbidity risk	EuroSCORE	ICU time (hours)	Status
CS_01	Male	48	CAB	0,0324	0,7585	20,95	Urgent
CS_02	Female	71	Valve + Other	0,1007	3,1299	35,67	Elective
CS_03	Male	68	CAB	0,1170	5,5840	24,28	Urgent
CS_04	Male	69	CAB	0,0566	0,7158	41,22	Elective
CS_05	Male	69	Valve	0,0538	0,9732	27,23	Elective
CS_07	Male	73	CAB + Valve	0,1437	4,4838	21,32	Elective
CS_08	Male	63	CAB	0,1185	2,7970	46,28	Urgent
CS_09	Male	80	CAB	0,0658	1,1776	28,17	Elective
CS_10	Male	78	CAB	0,0643	1,8081	122,30	Urgent
CS_11	Male	58	Valve	-	5,5562	46,78	Urgent
CS_12	Male	51	Other	-	0,5581	30,02	Elective
CS_13	Male	80	CAB	0,2439	2,6446	52,53	Urgent
CS_14	Male	82	CAB + Valve	0,1015	2,5537	24,10	Elective
CS_15	Male	84	CAB	0,0950	2,1180	26,47	Urgent

Table B.2: Adjustment performed for manual synchronization for each patient.

Patient	**Adjustment for manual synchronization (seconds)**
CS_01	+42,00
CS_02	+76,00
CS_03	+80,00
CS_04	+73,00
CS_05	+110,00
CS_07	+126,00
CS_08	+143,00
CS_09	+146,00
CS_10	-10,00
CS_11	-13,00
CS_12	-11,00
CS_13	+8,00
CS_14	-1,00
CS_15	0,00

Table B.3: Correspondence between patients and segments and the respective lengths.

Patient	**Number of points**		**Segment**	**Number of points**	
	IABP	**Nexfin**		**IABP**	**Nexfin**
CS_01	2028	1926	0	693	641
			1	669	642
			2	664	642
CS_02	1309	1302	3	734	616
			4	654	612
CS_03	3386	3259	5	748	700
			6	719	700
			7	723	700
			8	720	700
CS_04	1382	1229	9	739	610
			10	634	610
CS_05	2689	2296	11	853	700
			12	819	700
			13	811	700
CS_07	4251	4162	14	712	700
			15	710	700
			16	711	700
			17	714	700
			18	713	700
			19	684	656
CS_08	4882	4675	20	746	700
			21	722	700
			22	731	700
			23	735	700
			24	725	700
			25	684	656
CS_09	662	658	26	661	657
CS_10	997	852	27	825	700
CS_11	1404	1147	28	853	700
CS_12	1004	979	29	718	700
CS_13	988	956	30	707	700
CS_14	717	675	31	716	674
CS_15	1122	1087	32	726	700

Appendix C

Results: Complementary plots

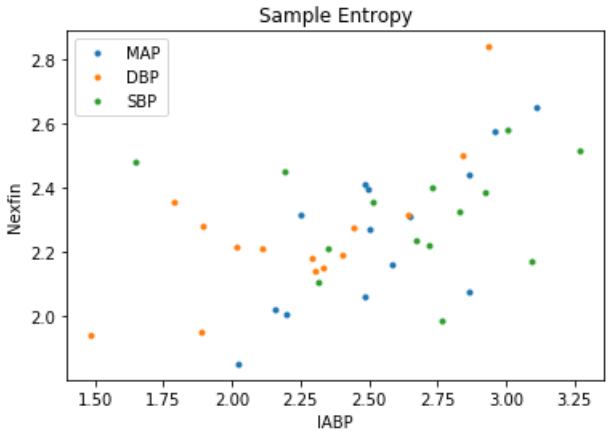

Figure C.1: Sample entropy for MAP, DBP and SBP: IABP vs Nexfin

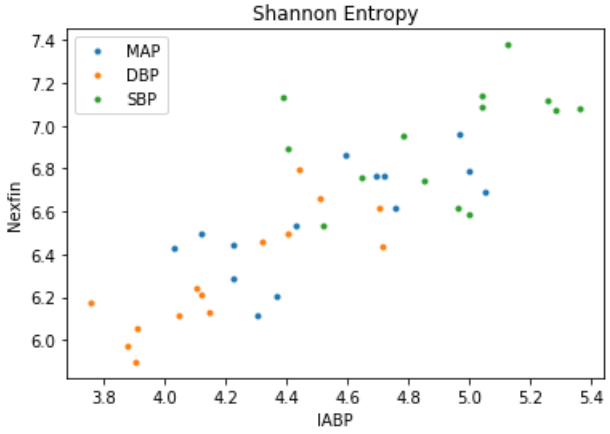

Figure C.2: Shannon entropy for MAP, DBP and SBP: IABP vs Nexfin

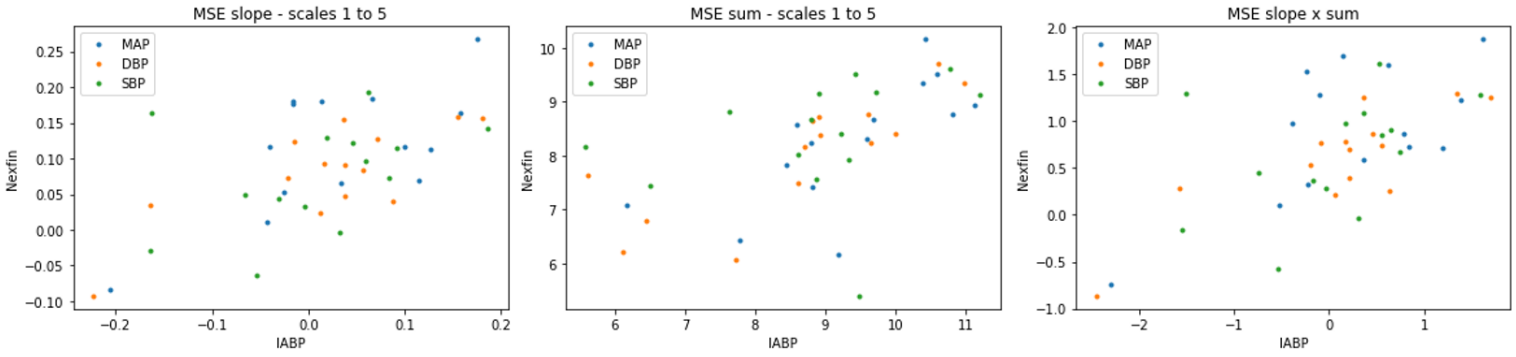

Figure C.3: MSE_{slope}, MSE_{Σ} and $MSE_{slope \cdot \Sigma}$ (scales 1 to 5) for the three signals (MAP, DBP, SBP) comparing the two methods: IABP and Nexfin

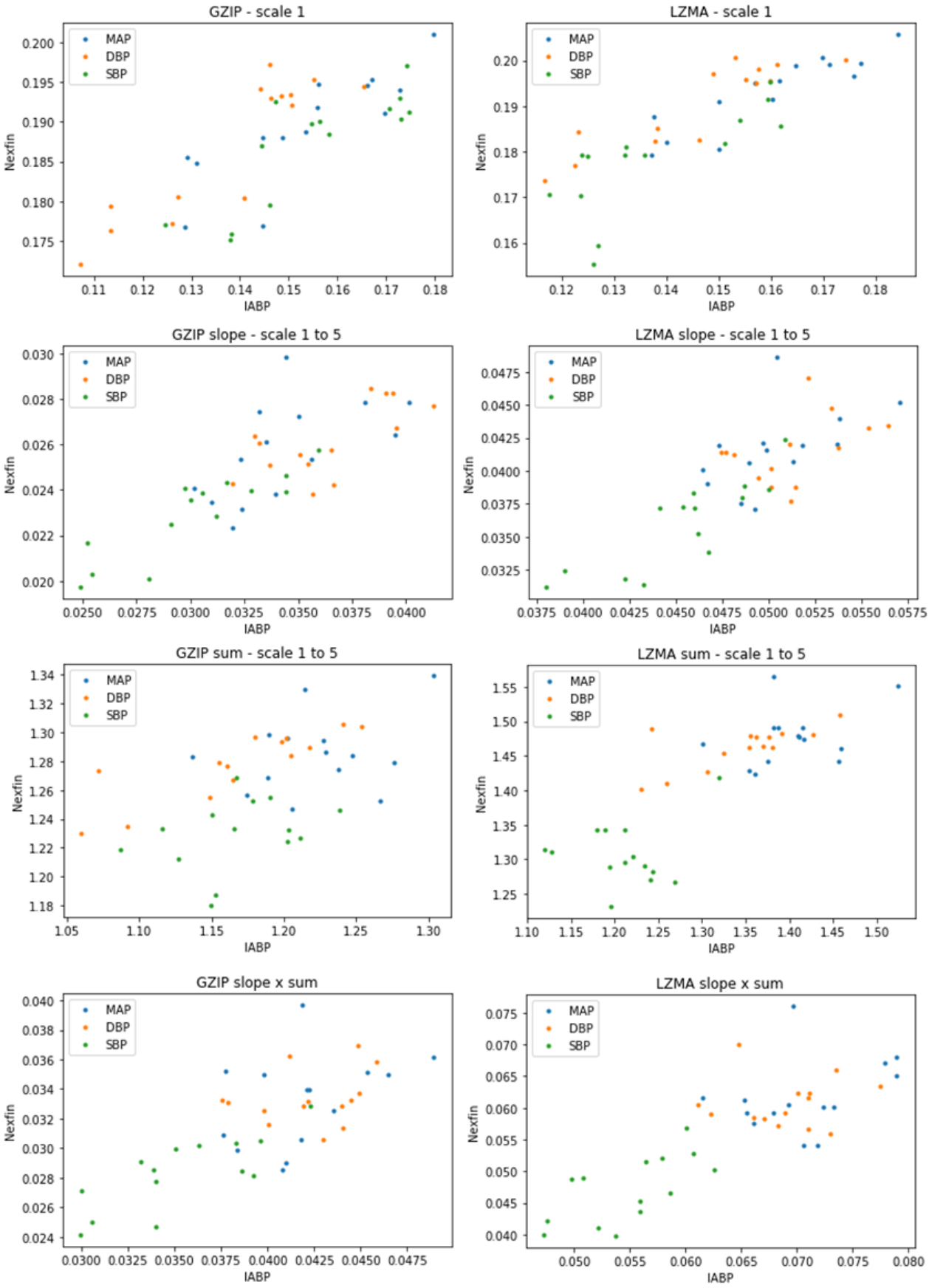

Figure C.4: MSC_{slope}, MSC_{Σ} and $MSC_{slope \cdot \Sigma}$ (scales 1 to 5) for the three signals (MAP, DBP, SBP) and the two compressors (GZIP and LZMA) comparing the two methods: IABP and Nexfin

Appendix D

Results: Linear regression tables

Table D.1: Linear regression standardized coefficients and 95% CI for the association between frequency and entropy measures, and the logaritmically transformed time spent in the ICU for each blood pressure signal. P-values in bold are lower than 0.05.

	Coefficient (95% CI)			
	log10 STS risk			
	IABP		**Nexfin®**	
HF				
MAP	0.13 (-0.56, 0.83)	0.678	-0.04 (-0.59, 0.50)	0.862
DBP	0.16 (-0.65, 0.97)	0.681	-0.02 (-0.58, 0.55)	0.948
SBP	0.00 (-0.49, 0.50)	0.991	-0.05 (-0.48, 0.38)	0.803
MF				
MAP	-0.07 (-0.90, 0.76)	0.847	-0.08 (-0.65, 0.49)	0.760
DBP	0.04 (-0.93, 1.01)	0.934	-0.15 (-0.79, 0.50)	0.629
SBP	0.04 (-0.45, 0.53)	0.847	0.05 (-0.45, 0.55)	0.839
Shannon				
MAP	-1.03 (-3.03, 0.96)	0.279	-3.12 (-5.88, -0.36)	0.030
DBP	-1.04 (-3.12, 1.04)	0.294	-2.11 (-4.66, 0.44)	0.096
SBP	-0.24 (-2.32, 1.84)	0.805	-1.66 (-4.33, 1.01)	0.198
SampEn				
MAP	-1.06 (-3.15, 1.04)	0.290	-0.28 (-3.04, 2.48)	0.827
DBP	0.05 (-1.53, 1.63)	0.950	2.63 (-0.24, 5.51)	0.069
SBP	-1.20 (-2.75, 0.36)	0.119	2.88 (-0.93, 6.69)	0.125
MSE_{slope}				
MAP	-5.25 (-11.82, 1.33)	0.107	0.19 (-7.39, 7.78)	0.957
DBP	-2.19 (-8.32, 3.94)	0.448	-2.56 (-12.26, 7.14)	0.573
SBP	-0.14 (-6.74, 6.45)	0.963	1.26 (-8.5, 11.02)	0.782
MSE_{Σ}				
MAP	-0.24 (-0.71, 0.24)	0.296	0.02 (-0.55, 0.59)	0.947
DBP	-0.05 (-0.48, 0.38)	0.805	0.26 (-0.35, 0.87)	0.370
SBP	-0.33 (-0.77, 0.11)	0.130	0.20 (-0.39, 0.80)	**0.465**
$MSE_{slope \cdot \Sigma}$				
MAP	-0.47 (-1.14, 0.20)	0.153	0.03 (-0.91, 0.97)	0.942
DBP	-0.24 (-0.86, 0.39)	0.429	-0.27 (-1.48, 0.94)	0.634
SBP	0.03 (-0.71, 0.76)	0.941	0.18 (-1.00, 1.36)	0.744

Abbreviations: IABP, invasive arterial blood pressure; MAP, mean arterial blood pressure; DBP, diastolic blood pressure; SBP, systolic blood pressure; CI, confidence interval; ICU, intensive care unit; MSE, multiscale entropy; SampEn, sample entropy; MF, mid-frequency; HF, high frequency.

Table D.2: Linear regression standardized coefficients and 95% CI for the association between frequency and compression measures, and the logaritmically transformed STS risk score for each blood pressure signal. P-values in bold are lower than 0.05.

	Coefficient (95% CI)			
	log10 STS risk			
	IABP		**Nexfin®**	
HF				
MAP	-0.24 (-0.93, 0.46)	0.468	-0.14 (-0.71, 0.43)	0.590
DBP	0.28 (-0.51, 1.07)	0.447	-0.24 (-0.82, 0.35)	0.388
SBP	-0.13 (-0.65, 0.40)	0.604	-0.09 (-0.52, 0.33)	0.635
MF				
MAP	0.24 (-0.60, 1.07)	0.543	-0.04 (-0.65, 0.57)	0.890
DBP	0.64 (-0.37, 1.65)	0.191	-0.25 (-0.90, 0.40)	0.409
SBP	0.02 (-0.46, 0.50)	0.917	-0.02 (-0.60, 0.57)	0.946
$GZIP_{scale1}$				
MAP	22.74 (-16.85, 62.32)	0.230	-6.88 (-102.92, 89.17)	0.876
DBP	7.95 (-27.64, 43.55)	0.629	29.88 (-47.07, 106.83)	0.407
SBP	38.21 (-5.89, 82.30)	0.082	48.68 (-48.40, 145.76)	0.290
$GZIP_{slope}$				
MAP	-182.23 (-420.81, 56.35)	0.120	-153.89 (-460.82, 153.04)	0.290
DBP	-48.47 (-265.25, 168.31)	0.629	-214.63 (-687.73, 258.48)	0.336
SBP	-155.18 (-373.91, 63.56)	0.145	-349.96 (-729.11, 29.19)	0.067
$GZIP_{\Sigma}$				
MAP	4.99 (-9.46, 19.43)	0.459	-13.98 (-37.59, 9.63)	0.216
DBP	2.04 (-8.69, 12.78)	0.680	4.27 (-22.45, 31.00)	0.729
SBP	9.63 (-6.32, 25.59)	0.208	0.85 (-25.50, 27.20)	0.944
$GZIP_{slope \cdot \Sigma}$				
MAP	-148.82 (-368.22, 70.57)	0.162	-122.95 (-336.07, 90.17)	0.228
DBP	-35.88 (-273.71, 201.95)	0.744	-219.44 (-629.71, 190.84)	0.261
SBP	-131.11 (-324.09, 61.86)	0.161	-307.01 (-582.38, -31.64)	**0.032**
$LZMA_{scale1}$				
MAP	23.04 (-19.65, 65.72)	0.257	8.94 (-73.05, 90.94)	0.813
DBP	5.00 (-32.45, 42.45)	0.772	18.70 (-53.30, 90.70)	0.576
SBP	24.30 (-20.99, 69.59)	0.260	3.97 (-57.09, 65.03)	0.888
$LZMA_{slope}$				
MAP	-168.35 (-412.99, 76.28)	0.156	-176.76 (-392.97, 39.45)	0.099
DBP	-99.08 (-325.72, 127.55)	0.353	-162.87 (-437.36, 111.62)	0.216
SBP	-153.05 (-348.97, 42.87)	0.112	-211.72 (-419.88, -3.56)	**0.047**
$LZMA_{\Sigma}$				
MAP	2.00 (-9.53, 13.53)	0.708	-9.13 (-24.28, 6.02)	0.209
DBP	0.08 (-9.33, 9.48)	0.986	-1.71 (-22.11, 18.68)	0.855
SBP	0.91 (-11.12, 12.95)	0.870	-8.54 (-22.39, 5.31)	0.199
$LZMA_{slope \cdot \Sigma}$				
MAP	-57.31 (-182.59, 67.97)	0.332	-93.56 (-203.53, 16.41)	0.087
DBP	-55.15 (-194.26, 83.97)	0.398	-100.58 (-276.07, 74.9)	0.230
SBP	-81.27 (-225.05, 62.50)	0.236	-152.08 (-281.28, -22.88)	**0.025**

Abbreviations: IABP, invasive arterial blood pressure; MAP, mean arterial blood pressure; DBP, diastolic blood pressure; SBP, systolic blood pressure; CI, confidence interval; STS, society of thoracic surgeons; MF, mid-frequency; HF, high frequency.

Table D.3: Linear regression standardized coefficients and 95% CI for the association between entropy and frequency measures, and the logaritmically transformed EUROScore for each blood pressure signal. P-values in bold are lower than 0.05.

	log10 EUROScore			
	Coefficient (95% CI)			
	IABP		**Nexfin®**	
HF				
MAP	-0.37 (-1.03, 0.28)	0.238	-0.23 (-0.75, 0.28)	0.341
DBP	0.53 (-0.24, 1.30)	0.157	-0.28 (-0.82, 0.25)	0.270
SBP	-0.19 (-0.65, 0.28)	0.406	-0.20 (-0.58, 0.18)	0.274
MF				
MAP	-0.14 (-0.91, 0.64)	0.705	-0.33 (-0.85, 0.19)	0.193
DBP	0.02 (-0.90, 0.94)	0.963	-0.41 (-1.00, 0.18)	0.158
SBP	0.03 (-0.42, 0.49)	0.876	-0.31 (-0.75, 0.14)	0.161
Shannon				
MAP	0.18 (-1.59, 1.96)	0.826	1.12 (-1.25, 3.50)	0.323
DBP	0.77 (-1.18, 2.73)	0.405	1.63 (-0.57, 3.84)	0.132
SBP	0.37 (-1.52, 2.27)	0.674	1.64 (-0.75, 4.03)	0.161
SampEn				
MAP	1.37 (-0.51, 3.26)	0.137	0.89 (-1.73, 3.50)	0.474
DBP	0.61 (-0.87, 2.08)	0.388	0.98 (-1.74, 3.70)	0.447
SBP	0.44 (-1.01, 1.88)	0.522	0.72 (-2.87, 4.30)	0.671
MSE_{slope}				
MAP	-2.23 (-8.18, 3.72)	0.431	-4.51 (-11.36, 2.35)	0.177
DBP	-3.86 (-9.49, 1.77)	0.161	-6.02 (-14.94, 2.89)	0.167
SBP	-2.76 (-9.01, 3.49)	0.354	-3.99 (-12.05, 4.07)	0.302
MSE_{Σ}				
MAP	0.11 (-0.34, 0.56)	0.598	0.13 (-0.40, 0.65)	0.612
DBP	0.02 (-0.35, 0.39)	0.907	0.13 (-0.43, 0.68)	0.629
SBP	0.14 (-0.26, 0.55)	0.462	0.01 (-0.54, 0.56)	0.956
$MSE_{slope \cdot \Sigma}$				
MAP	-0.22 (-0.83, 0.38)	0.437	-0.52 (-1.38, 0.33)	0.206
DBP	-0.40 (-0.97, 0.18)	0.158	-0.77 (-1.86, 0.31)	0.146
SBP	-0.26 (-0.95, 0.43)	0.433	-0.52 (-1.49, 0.45)	0.265

Abbreviations: IABP, invasive arterial blood pressure; MAP, mean arterial blood pressure; DBP, diastolic blood pressure; SBP, systolic blood pressure; CI, confidence interval; MSE, multiscale entropy; SampEn, sample entropy.

Table D.4: Linear regression standardized coefficients and 95% CI for the association between the compression measures and the logaritmically transformed EUROScore for each blood pressure signal. P-values in bold are lower than 0.05.

	log10 EUROScore			
	Coefficient (95% CI)			
	IABP		**Nexfin®**	
$GZIP_{scale1}$				
MAP	7.88 (-28.57, 44.33)	0.646	-27.25 (-115.45, 60.95)	0.514
DBP	3.07 (-31.09, 37.23)	0.848	14.61 (-54.32, 83.53)	0.653
SBP	11.11 (-26.18, 48.40)	0.528	30.04 (-54.57, 114.66)	0.454
$GZIP_{slope}$				
MAP	-31.59 (-229.48, 166.30)	0.734	-17.70 (-294.57, 259.18)	0.892
DBP	-26.37 (-237.78, 185.04)	0.790	-42.56 (-423.94, 338.82)	0.812
SBP	-40.58 (-212.49, 131.34)	0.616	-21.98 (-348.75, 304.78)	0.886
$GZIP_{\Sigma}$				
MAP	1.64 (-12.17, 15.45)	0.800	-11.52 (-34.44, 11.41)	0.295
DBP	0.58 (-9.59, 10.74)	0.904	0.69 (-24.64, 26.02)	0.954
SBP	4.40 (-10.41, 19.21)	0.530	6.60 (-17.95, 31.14)	0.569
$GZIP_{slope \cdot \Sigma}$				
MAP	-23.47 (-207.45, 160.51)	0.786	-30.80 (-222.69, 161.09)	0.733
DBP	-27.65 (-254.79, 199.50)	0.795	-61.78 (-393.01, 269.46)	0.692
SBP	-39.58 (-196.32, 117.16)	0.592	-39.11 (-283.32, 205.10)	0.733
$LZMA_{scale1}$				
MAP	7.29 (-32.54, 47.11)	0.697	-7.00 (-81.75, 67.75)	0.842
DBP	0.66 (-35.29, 36.61)	0.969	7.00 (-58.44, 72.45)	0.820
SBP	9.91 (-28.23, 48.05)	0.582	0.74 (-53.28, 54.76)	0.977
$LZMA_{slope}$				
MAP	-31.65 (-233.51, 170.22)	0.739	-54.4 (-256.24, 147.43)	0.568
DBP	-103.93 (-324.02, 116.16)	0.324	-32.82 (-270.67, 205.02)	0.769
SBP	-83.51 (-242.67, 75.64)	0.275	-44.21 (-222.47, 134.05)	0.599
$LZMA_{\Sigma}$				
MAP	0.54 (-10.68, 11.77)	0.918	-6.82 (-21.63, 7.99)	0.335
DBP	-1.15 (-10.20, 7.91)	0.788	-1.00 (-20.75, 18.74)	0.914
SBP	-0.37 (-12.02, 11.28)	0.946	-2.82 (-16.28, 10.64)	0.656
$LZMA_{slope \cdot \Sigma}$				
MAP	-20.49 (-133.55, 92.57)	0.700	-39.27 (-143.33, 64.80)	0.427
DBP	-71.21 (-206.03, 63.62)	0.272	-21.75 (-177.14, 133.64)	0.766
SBP	-57.10 (-180.57, 66.37)	0.334	-37.02 (-150.60, 76.56)	0.491

Abbreviations: IABP, invasive arterial blood pressure; MAP, mean arterial blood pressure; DBP, diastolic blood pressure; SBP, systolic blood pressure; CI, confidence interval.